12

SUBBAND ADAPTIVE FILTERS

12.1 INTRODUCTION

There are many applications where the required adaptive-filter order is high, as for example, in acoustic echo cancellation where the unknown system (echo) model has a long impulse response, on the order of a few thousand samples [1]-[5]. In such applications, the adaptive-filtering algorithm entails a large number of computations. In addition, the high order of the adaptive filter affects the convergence speed.

A solution to problems where long-impulse-response filters are needed is to employ adaptive filtering in subbands. In subband adaptive filtering, both the input signal and the desired signal are split into frequency subbands via an analysis filter bank. Assuming that the signal decomposition in subchannels is effective, we can decimate (subsample) these subband signals and apply adaptive filtering to the resulting signals. Each subband adaptive filter usually has shorter impulse response than its fullband counterpart. If a gradient type algorithm is used to update the adaptive filters, we can adjust the step size in the adaptation algorithm individually for each subband, which leads to higher convergence speed than in the case of fullband adaptive filter.

Decimation allows the reduction in computational complexity. Mainly if critical subsampling (i.e., decimation by a factor equal to the number of subbands) is employed, aliasing effects may impair the obtained filter estimates. This issue will be discussed during this chapter. Therefore, by judicious use of adaptive filtering in subbands we can reduce the computational complexity, as well as increase the algorithm convergence speed [1]-[7].

This chapter starts with a brief introduction to multirate systems, where the concepts of decimation, interpolation, and filter banks are presented. Then, the basic structures for adaptive filtering in subbands are presented along with a discussion regarding their main features. The concept of delayless subband adaptive filtering is also addressed, where the adaptive-filter coefficients are updated in subbands and mapped to an equivalent fullband filter. Finally, we point out the relation between subband and block adaptive-filtering (also known as frequency-domain adaptive filters) algorithms.

P.S.R. Diniz, *Adaptive Filtering*, DOI: 10.1007/978-0-387-68606-6_12,

12.2 MULTIRATE SYSTEMS

In this section, we briefly review the fundamentals of multirate systems which are essential to implement adaptive filters in subbands. For further details related to multirate systems and filter banks the reader can refer to the review article [8] or the comprehensive textbook [9].

12.2.1 Decimation and Interpolation

Decimation (also known as down-sampling or compression) of a digital signal $x(k)$ by a factor of L means reducing its sampling rate L times. Decimation is achieved by retaining only every Lth sample of the signal. The decimator symbol is depicted in Fig. 12.1.a.

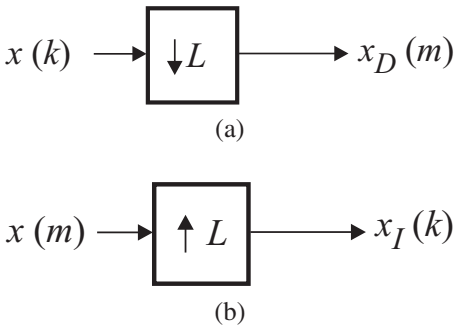

Figure 12.1 (a) Decimation by a factor L, (b) Interpolation by a factor L.

The decimated signal is then $x_D(m) = x(mL)$. In the frequency domain, if the spectrum of $x(k)$ is $X(\mathrm{e}^{\jmath\omega})$, the spectrum of the sub-sampled signal, $X_D(\mathrm{e}^{\jmath\omega})$ is given by [9]

$$X_D(\mathrm{e}^{\jmath\omega}) = \frac{1}{L}\sum_{k=0}^{L-1} X(\mathrm{e}^{\jmath\frac{\omega-2\pi k}{L}}) \tag{12.1}$$

The above equation indicates that the spectrum of $x_D(m)$ is composed of copies of the spectrum of $x(k)$ expanded by L and repeated with period 2π. Figs. 12.2.a and 12.2.b depict the effect of sub-sampling on the spectrum of $x(k)$, for $L = 2$. This implies that, in order to avoid aliasing after sub-sampling, the bandwidth of the signal $x(k)$ must be limited to the interval $[-\frac{\pi}{L}, \frac{\pi}{L}]$. In fact, the sub-sampling operation is generally preceded by a lowpass filter that approximates the following frequency response

$$H_D(\mathrm{e}^{\jmath\omega}) = \begin{cases} 1, & \omega \in [-\frac{\pi}{L}, \frac{\pi}{L}] \\ 0, & \text{otherwise} \end{cases} \tag{12.2}$$

It should be noted that the decimation operation is shift varying, i.e., if the input signal $x(k)$ is shifted, the output signal will not in general be a shifted version of the previous output. More precisely, the decimation is a periodically shift-invariant operation.

The interpolation (or up-sampling) of a digital signal $x(m)$ by a factor of L entails including $L-1$ zeros in between samples. The interpolator symbol is depicted in Fig. 12.1.b.

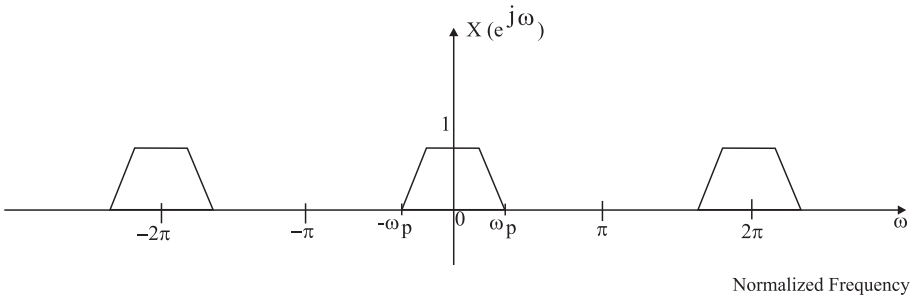

(a) Original spectrum

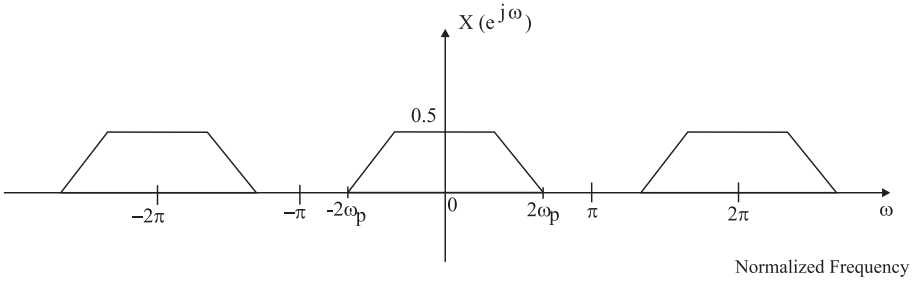

(b) Spectrum of a down-sampled signal

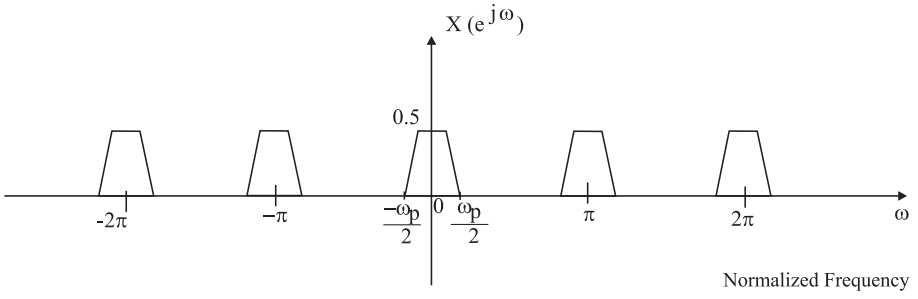

(c) Spectrum of an up-sampled signal

Figure 12.2 Spectra of up- and down-sampled signals.

The interpolated signal is then

$$x_I(k) = \begin{cases} x(\frac{k}{L}), & k = mL, m \in \mathcal{Z} \\ 0, & \text{otherwise} \end{cases} \tag{12.3}$$

If the spectrum of $x(m)$ is $X(\mathrm{e}^{\jmath\omega})$, it is straightforward to show that the spectrum of the up-sampled signal, $X_I(\mathrm{e}^{\jmath\omega})$, is given by

$$X_I(\mathrm{e}^{\jmath\omega}) = X(\mathrm{e}^{\jmath\omega L}) \tag{12.4}$$

Since the spectrum of the input signal is periodic with period 2π, the spectrum of the interpolated signal will have period $\frac{2\pi}{L}$. Fig. 12.2.c illustrates how the signal spectrum is modified after the

up-sampling operation. If we wish to obtain a smooth interpolated version of $x(m)$, the spectrum of the interpolated signal must have the same shape of the spectrum of $x(m)$. This can be obtained by filtering out the repetitions of the spectra beyond $[-\frac{\pi}{L}, \frac{\pi}{L}]$. Thus, the up-sampling operation is generally followed by a lowpass filter which approximates the following frequency response

$$H_I(\mathrm{e}^{\jmath\omega}) = \begin{cases} L, & \omega \in [-\frac{\pi}{L}, \frac{\pi}{L}] \\ 0, & \text{otherwise} \end{cases} \tag{12.5}$$

The decimator and interpolator blocks are fundamental to represent (or implement) serial-to-parallel and parallel-to-serial converters. That is, given a signal $x(k)$ whose samples appear serially, we can transform this sequence into blocks of length L by using delay operators and decimators whose representation is depicted in Fig. 12.3.a. The signal block at the output retains L consecutive samples of the input signal as follows

$$\mathbf{x}(m) = [x(mL)\, x(mL-1) \ldots x(mL-L+1)]^T \tag{12.6}$$

This notation is slightly different from the one to be used in the remaining chapters, since m here denotes the block number and not the index of the most recent element of $\mathbf{x}(m)$. In this chapter we will use the *block* notation because it leads to simpler description of the algorithms. The implementation of the serial-to-parallel converter in terms of decimators and delays is further illustrated in Fig. 12.3.b.

On the other hand, given a block signal $\mathbf{x}(m)$, we can transform the parallel data of length L back into a delayed serial data as shown in Fig. 12.4.a. The implementation of the parallel-to-serial converter in terms of interpolators and delays is illustrated in Fig. 12.4.b.

12.3 FILTER BANKS

In subband adaptive filtering as well as in a number of other applications, it is advantageous to split a sequence $x(k)$ into several frequency bands. This is illustrated on the left-hand side of Fig. 12.5.

The analysis filters, represented by the transfer functions $F_i(z)$ for $i = 0, 1, \ldots, M-1$, comprise of a lowpass filter $F_0(z)$, bandpass filters $F_i(z)$ for $i = 1, 2, \ldots, M-2$, and a highpass filter $F_{M-1}(z)$. Ideally these filters have nonoverlapping passbands, while they together cover the entire spectrum of the input signal. Since each of the analysis filter outputs $x_i(k)$, $i = 0, 1, \ldots, M-1$ has the same number of samples as the original signal $x(k)$, after the M-band decomposition, all signals $x_i(k)$ together have M times more samples than the original one. This expansion on the number of samples is undesirable because of the resulting computational burden.

In most cases, the input signal is uniformly split into subbands, where each of the frequency bands has the same bandwidth. Since the bandwidth of each analysis filter output band is M times smaller than in the original signal, we can decimate each $x_i(k)$ by a factor of L smaller or equal to M without destroying the original information. For $L = M$, the amount of data after the decimators in Fig. 12.5 is maintained when compared to the number of samples of the input signal. This case is called

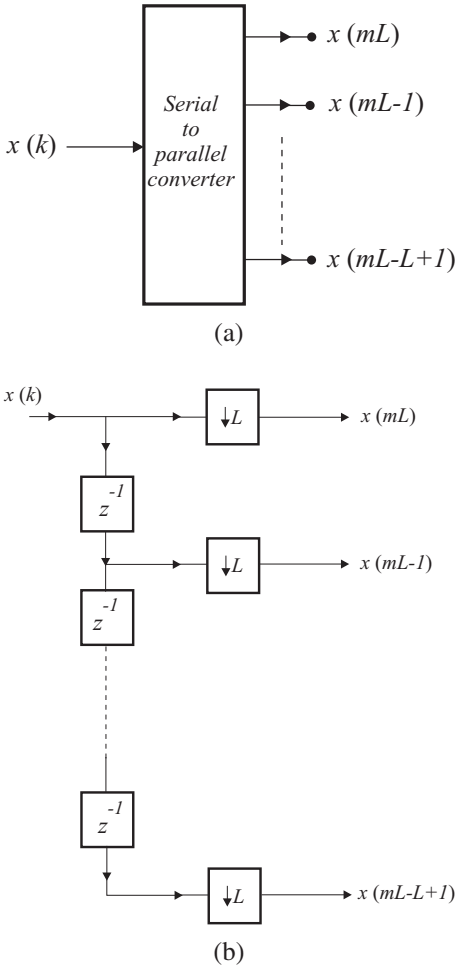

Figure 12.3 Serial-to-parallel converter (a) Symbol, (b) Implementation.

maximally (or critically) decimated analysis filter bank. If $L > M$, there is a loss of information due to aliasing which does not allow the recovery of the original signal. For $L \leq M$, it is possible to retain all information contained in the input signal by properly designing the analysis filters in conjunction with the synthesis filters $G_i(z)$, for $i = 0, 1, \ldots, M-1$. If no signal processing task is performed in the subbands (see Fig. 12.5), the filter bank output $y(k)$ can be made to be a delayed version of the input signal $x(k)$, where the delay is due to the causality of the subband filters. In this case, we have a perfect reconstruction filter bank. In fact, there are several methods for designing the analysis filters $F_i(z)$ and the synthesis filters $G_i(z)$ such that perfect reconstruction is achieved or arbitrarily approximated. These filters can be finite-length (FIR) filters with overlapping frequency responses, which are designed to cancel out the aliasing effects and results in the perfect reconstruction.

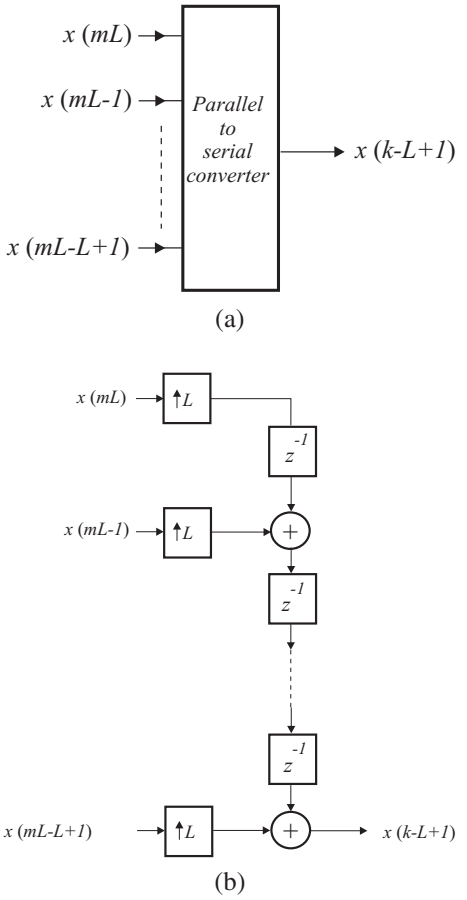

Figure 12.4 Parallel-to-serial converter (a) Symbol, (b) Implementation.

In the case where $L < M$, the filter bank is called oversampled (or noncritically sampled) since we are retaining more samples in the subbands than the input signal. Oversampled filter banks appear frequently in subband adaptive-filtering applications, however their design is beyond the scope of this book.

We will now discuss the polyphase representation of a transfer function which is quite useful in describing filter banks. Defining $E_{ij}(z) = \sum_{l=0}^{N_p-1} f_i(Ll + j)z^{-l}$ as the polyphase components of the analysis filter $F_i(z)$, and N_p as the length of the polyphase components of the analysis filters, we can express the transfer function of the filter $F_i(z)$ as follows

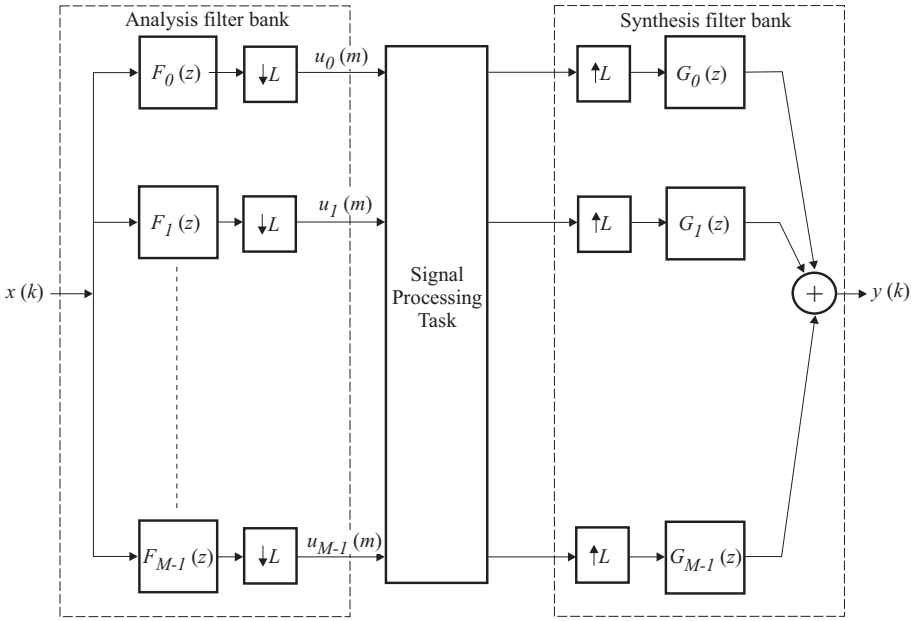

Figure 12.5 Signal processing in subbands.

$$
\begin{aligned}
F_i(z) &= \sum_{k=0}^{N_pL-2L+1} f_i(k)z^{-k} \\
&= \sum_{l=0}^{N_p-1} f_i(Ll)z^{-Ll} + z^{-1}\sum_{l=0}^{N_p-1} f_i(Ll+1)z^{-Ll} + \cdots + z^{-L+1}\sum_{l=0}^{N_p-1} f_i(Ll+L-1)z^{-Ll} \\
&= \sum_{j=0}^{L-1} z^{-j}E_{ij}(z^L) \qquad (12.7)
\end{aligned}
$$

In the polyphase decomposition we decompose each analysis filter $F_i(z)$ into L filters, the first one has an impulse response consisting of every sample of $f_i(k)$ whose indexes are multiples of L, the second one has every sample of $f_i(k)$ whose indexes are one plus a multiple of L, and so on. The resulting representation for an analysis subfilter, along with decimation, is depicted in Fig. 12.6. By means of a noble identity [9], the cascade connection of $E_{ij}(z^L)$ and the decimators can be replaced by decimators followed by the polynomials $E_{ij}(z)$.

For the synthesis filter bank we can employ an alternative polyphase decomposition which matches the interpolation operation. That is, each synthesis filter can be described in the following polyphase

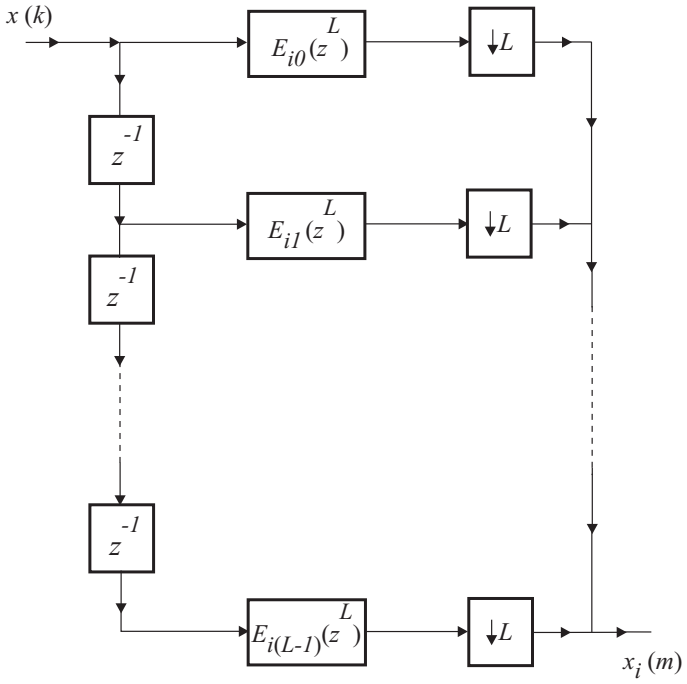

Figure 12.6 Polyphase representation.

form

$$G_i(z) = \sum_{j=0}^{M-1} z^{-(L-1-j)} R_{ji}(z^L) \tag{12.8}$$

Again by means of a noble identity [9], the polynomials $R_{ji}(z^L)$ preceded by interpolators can be replaced by interpolators preceded by the polynomials $R_{ji}(z)$.

By replacing each of the filters $F_i(z)$ and $G_i(z)$ by their polyphase components, the M-band filter bank of Fig. 12.5 can be transformed in the structure of Fig. 12.7. The matrices $\mathbf{E}(z)$ and $\mathbf{R}(z)$ are formed from the polyphase components of $F_i(z)$ and $G_i(z)$. $E_{ij}(z)$ is the jth polyphase component of $F_i(z)$ and $R_{ji}(z)$ is the jth polyphase component of $G_i(z)$. From Fig. 12.7 we conclude that if $\mathbf{R}(z)\mathbf{E}(z) = z^{-\Delta}\mathbf{I}$, where Δ is an arbitrary delay and $\mathbf{I}$ is the identity matrix, the M-band filter bank holds the perfect reconstruction property.

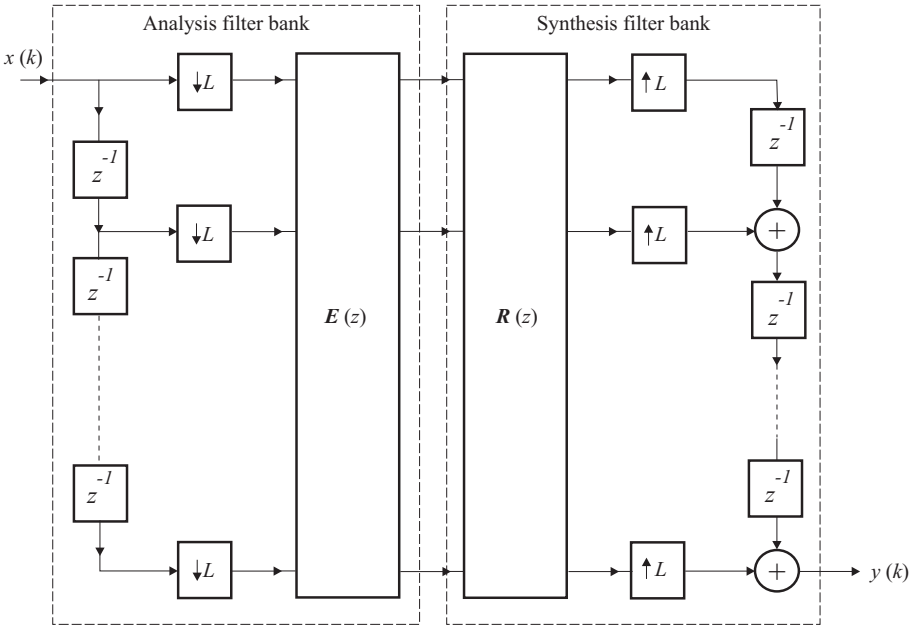

Figure 12.7 M-band filter bank with polyphase representation.

12.3.1 Two-Band Perfect Reconstruction Filter Banks

For a two-band perfect reconstruction filter bank with FIR analysis and synthesis filters, the following conditions must be satisfied

$$F_0(-z)F_1(z) - F_0(z)F_1(-z) = 2cz^{-2l-1} \tag{12.9}$$

$$G_0(z) = -\frac{z^{2(l-\Delta)}}{c}F_1(-z) \tag{12.10}$$

$$G_1(z) = \frac{z^{2(l-\Delta)}}{c}F_0(-z) \tag{12.11}$$

where equation (12.9) guarantees that the synthesis filters are FIR, while equations (12.10) and (12.11) guarantee perfect reconstruction. The delay Δ is included in equations (12.10) and (12.11) in order to guarantee that the subfilters in the filter bank are causal.

Equations (12.9) to (12.11) lead to the following design procedure for the two-band perfect reconstruction filter bank [10]: (1) Find a polynomial $P(z)$ such that $P(-z) - P(z) = 2z^{-2l-1}$; (2) Factorize $P(z)$ into two factors, $F_0(z)$ and $F_1(-z)$, such that $F_0(z)$ and $F_1(-z)$ are lowpass filters; (3) Design $G_0(z)$ and $G_1(z)$ using equations (12.10) and (12.11). In step (1) $P(z)$ is an approximation to a half-band filter[1], whose amplitude response should be positive everywhere. In case this

[1]The amplitude response of a half-band filter is symmetric with respect to $\frac{\pi}{2}$, with $\omega_p + \omega_s = \pi$, where ω_p is the passband edge and ω_s is the stopband edge.

condition is not initially satisfied in the design, we should add δz^{-2l-1} to $P(z)$ such that δ is the modulus of the smallest (negative) value of the designed $P(z)$. We add that the factorization step (2) becomes ill-conditioned when designing high-order filters. In this case, alternative design methods can be employed [9].

In some applications, it is desired that the filter bank be made up of linear-phase filters. In this case, one has to find a linear-phase product filter $P(z)$, and perform linear-phase factorizations of it.

12.3.2 Analysis of Two-Band Filter Banks

From Fig. 12.5 we see that the signals after the analysis filters in a two-band filter bank are described by

$$X_i(z) = F_i(z)X(z) \quad \text{for} \quad i = 0, 1 \tag{12.12}$$

In the frequency domain, the decimated signals are

$$U_i(z) = \frac{1}{2}[X_i(z^{\frac{1}{2}}) + X_i(-z^{\frac{1}{2}})] \quad \text{for} \quad i = 0, 1 \tag{12.13}$$

Thus after interpolation of the $U_i(z)$, we get

$$\begin{aligned} U_i(z^2) &= \frac{1}{2}[X_i(z) + X_i(-z)] \\ &= \frac{1}{2}[F_i(z)X(z) + F_i(-z)X(-z)] \end{aligned} \tag{12.14}$$

The reconstructed signal is then expressed as

$$\begin{aligned} Y(z) &= G_0(z)U_0(z^2) + G_1(z)U_1(z^2) \\ &= \frac{1}{2}[F_0(z)G_0(z) + F_1(z)G_1(z)]X(z) + \frac{1}{2}[F_0(-z)G_0(z) + F_1(-z)G_1(z)]X(-z) \\ &= \frac{1}{2}\begin{bmatrix} X(z) & X(-z) \end{bmatrix}\begin{bmatrix} F_0(z) & F_1(z) \\ F_0(-z) & F_1(-z) \end{bmatrix}\begin{bmatrix} G_0(z) \\ G_1(z) \end{bmatrix} \end{aligned} \tag{12.15}$$

The last equality is called modulation-matrix representation of a two-band filter bank. In this case, the aliasing effect caused by the decimation operation is represented by the terms containing $X(-z)$.

Note that it is possible to avoid aliasing at the output by properly choosing the synthesis filter, as for example in the perfect reconstruction case.

12.3.3 Analysis of M-Band Filter Banks

The expression for two-band case can be easily generalized to M bands by noting that, after decimation by L, the signals will have $L-1$ aliased components. That is

$$X_d(z) = \frac{1}{L}\sum_{k=0}^{L-1} X(z^{\frac{1}{L}} \mathrm{e}^{-\frac{j2\pi k}{L}}) \tag{12.16}$$

The kth aliased component of $X(z)$ is $X(z^{\frac{1}{L}} \mathrm{e}^{-\jmath\frac{2\pi k}{L}})$.

Therefore, the modulation matrix for the M-band filter bank is given by

$$Y(z) = \frac{1}{2}\left[\begin{array}{cccc} X(z) & X(zW) & \ldots & X(zW^{L-1}) \end{array}\right] \left[\begin{array}{cccc} F_0(z) & F_1(z) & \ldots & F_{M-1}(z) \\ F_0(zW) & F_1(zW) & \ldots & F_{M-1}(zW) \\ \vdots & \vdots & \ddots & \vdots \\ F_0(zW^{L-1}) & F_1(zW^{L-1}) & \ldots & F_{M-1}(zW^{L-1}) \end{array}\right] \left[\begin{array}{c} G_0(z) \\ G_1(z) \\ \vdots \\ G_{M-1}(z) \end{array}\right] \tag{12.17}$$

where $W = \mathrm{e}^{-\jmath\frac{2\pi}{L}}$.

12.3.4 Hierarchical M-Band Filter Banks

By connecting two-band filter banks in series, we can produce many different kinds of maximally decimated decompositions. For example, we can design a 2^n-band uniform decomposition filter bank as illustrated in Fig. 12.8 for $n = 3$. It is also possible to implement nonuniform filter banks by using two-band filter banks in series, but using a different type of hierarchical decomposition [9]. A commonly used one is the octave-band decomposition.

12.3.5 Cosine-Modulated Filter Banks

Cosine-modulated filter banks are a class of filters efficient for the design and implementation of filter banks with large number of subbands. A cosine-modulated filter bank is easy to design because it is based on a single lowpass prototype filter whose impulse response satisfies some constraints required to achieve perfect reconstruction. It also leads to low computational complexity because the analysis and synthesis filter banks make use of the so-called discrete-time cosine transform (DCT), for which there are many fast implementations available for its computation.

The design of the maximally decimated cosine-modulated filter bank starts with a linear-phase prototype lowpass filter $F(z)$ whose passband edge is $\frac{\pi}{2L} - \delta$ and the stop-band edge is $\frac{\pi}{2L} + \delta$, where 2δ is the transition band. The length of the prototype filter is usually chosen to be an even multiple of the number of subbands: $N_{pr} = 2KL$, for K, an integer. Then, we generate cosine modulated versions of the prototype filter in order to obtain the analysis and synthesis filter banks. The impulse responses of the subfilters are given by

$$f_l(n) = 2f(n)\cos\left[(2l+1)\frac{\pi}{2L}\left(n - \frac{N_{pr}-1}{2}\right) + (-1)^l\frac{\pi}{4}\right] \tag{12.18}$$

$$g_l(n) = 2f(n)\cos\left[(2l+1)\frac{\pi}{2L}\left(n - \frac{N_{pr}-1}{2}\right) - (-1)^l\frac{\pi}{4}\right] \tag{12.19}$$

for $1 \leq n \leq N_{pr}$ and $0 \leq l \leq L-1$, where $f(n)$, for $n = 1, 2, \ldots, N_{pr}$, denotes the elements of the prototype impulse response. The constraints required to achieve perfect reconstruction are given

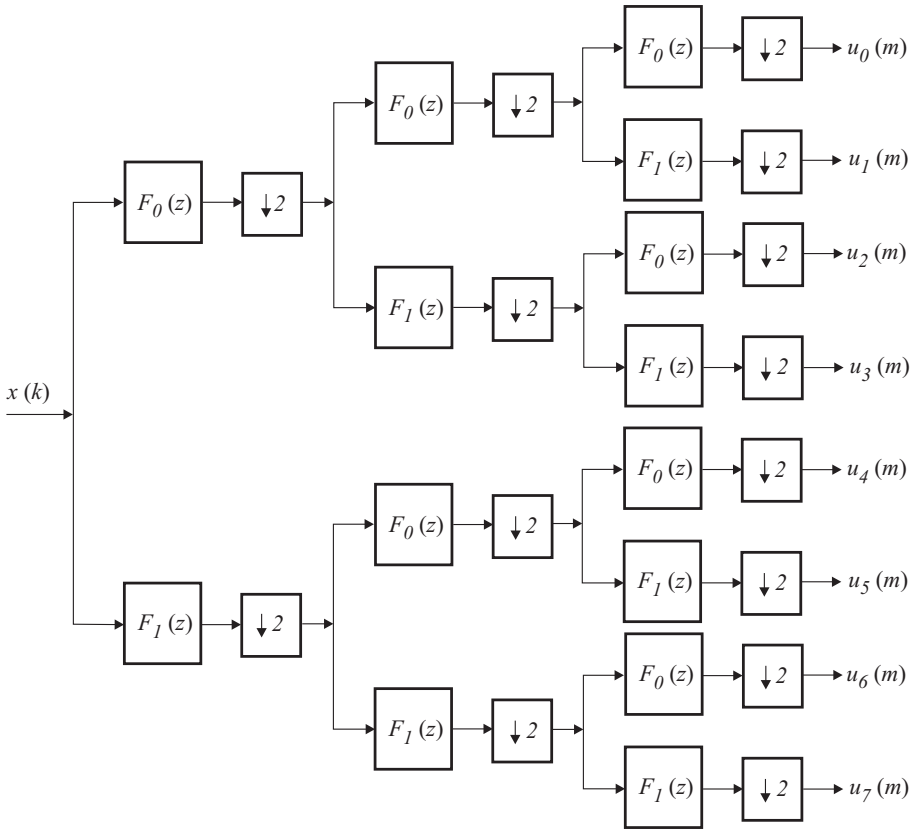

Figure 12.8 Hierarchical uniform filter bank.

by

$$E_j(z^{-1})E_j(z) + E_{j+L}(z^{-1})E_{j+L}(z) = \frac{1}{2L} \tag{12.20}$$

where $E_j(z)$ for any $j = 0, 1, \ldots, L-1$ is the jth polyphase component of the prototype filter $F(z)$.

There are computationally efficient implementations for the cosine-modulated filter bank which make use of the polyphase decomposition of the prototype filter. For further details refer to [9], [8]. Also, it is possible to design oversampled cosine-modulated filter banks with perfect reconstruction [11], which can be used in nonmaximally decimated subband adaptive filtering.

12.3.6 Block Representation

By using the polyphase concept we can show that any scalar linear time-invariant transfer function $H(z)$ can be implemented through a pseudocirculant matrix $\mathbf{H}(z)$, where the particular case of a 3×3 matrix $\mathbf{H}(z)$ is given by

$$\mathbf{H}(z) = \begin{bmatrix} H_0(z) & H_1(z) & H_2(z) \\ z^{-1}H_2(z) & H_0(z) & H_1(z) \\ z^{-1}H_1(z) & z^{-1}H_2(z) & H_0(z) \end{bmatrix} \tag{12.21}$$

where the $H_i(z)$, $i = 0, 1, 2$, are the polyphase components of $H(z)$.

The overall realization of $H(z)$ is equivalent to a cascade connection of the serial-to-parallel converter of Fig. 12.3.b, the transfer matrix $\mathbf{H}(z)$, and the parallel-to-serial converter of Fig. 12.4.b, except for a delay of z^{-L+1} since the converter of Fig. 12.4.b is causal (i.e., it utilizes negative powers of z). See the implementation of Fig. 12.7 with $\mathbf{H}(z)$ replacing the cascade of $\mathbf{E}(z)$ and $\mathbf{R}(z)$. This realization is known as blocked implementation of a scalar transfer function [32].

We note that the cascade of the unblock/block mechanisms of Figs. 12.4.b (noncausal case) and 12.4.a result in an identity matrix (see section 12.5). The reader is encouraged to verify this result.

12.4 SUBBAND ADAPTIVE FILTERS

A number of adaptive-filtering structures based on multirate techniques have been proposed in the literature [1]-[7], [14]-[28]. In most of these structures, the input signal is decomposed into subbands via an analysis filter bank, and the resulting signals are downsampled and filtered by adaptive filters. Each of these adaptive filters has order smaller than the equivalent full-band adaptive filter (by a factor approximately equal to the decimation rate). The subsampling operations create aliased versions of the decimated signal which will affect the performance of the adaptive filter. The aliasing effect is more severe when critically sampled filter banks are employed. An obvious solution is to allow frequency gaps between adjacent subbands, which for sure degrades the original signal quality. Some other structures apply subband decomposition only to the error signal in order to improve tracking ability in nonstationary environments [29]-[30].

Several adaptive subband structures have been suggested. One early approach uses pseudo-QMF[2] banks with overlapping subfilters and critical subsampling [1], i.e., with $L = M$. This results in undesirable aliased components at the output, which causes severe degradation. A second approach uses QMF banks with critical subsampling [2]. In order to avoid aliasing problems, it is shown that additional adaptive cross terms among the subbands are necessary. These cross terms, however, increase the computational complexity and reduce the convergence rate of the adaptive algorithm.

An alternative solution is to employ oversampling, that is, to use a decimation factor in the filtered signals smaller than the critical subsampling factor (or number of bands), i.e., with $L < M$. In the

[2] Quadrature-mirror filter.

oversampling case, the computational complexity is higher than needed because after decimation the number of samples retained in the subbands is larger than that of the filter bank input. Despite this problem, oversampled adaptive filters are often used in practice [3]-[7], [15]-[16]. In this chapter, we focus on the critically decimated case, although some analysis is also carried out for the general oversampled case.

In all subband structures above described, the convergence rate can be improved for colored input signals by using a normalized gradient algorithm in the update of the coefficients of each subband filter. This improvement is justified in Fig. 12.9, where considering that the filter bank consists of ideal subfilters, the spectrum of each signal in the subbands after critical decimation will be closer to that of white noise than that of the original fullband signal. If the spectral separation is perfect, the subband structure allows the transformation of the fullband adaptive-filtering problem into several independent narrowband adaptive-filtering subproblems. In general, the subband separation will be effective when the order of each subband adaptive filter is much smaller than the order of the fullband filter. The justification is that the speed of convergence becomes faster for all subbands, and the overall computational complexity is further reduced due to decimation.

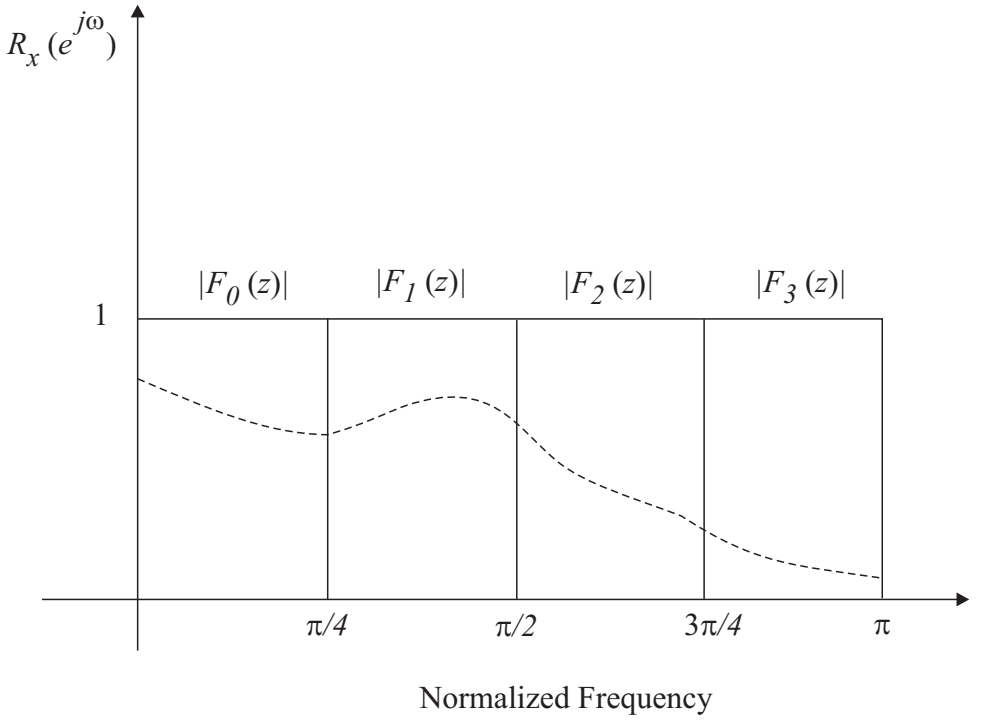

Figure 12.9 Spectrum split in subbands.

In the conventional subband adaptive filters, error signals are locally evaluated in each subband and an objective function taking into account all these local errors is minimized during adaptation. Fig. 12.10 illustrates the open-loop structure, where we can see that both input and reference signals are first split into subbands by an analysis filter bank. Then, the subband signals are filtered by an

adaptive-filter matrix in order to generate the output signals to be compared with the desired signals in the subbands. In the open-loop scheme, we aim to minimize the subband error energy.

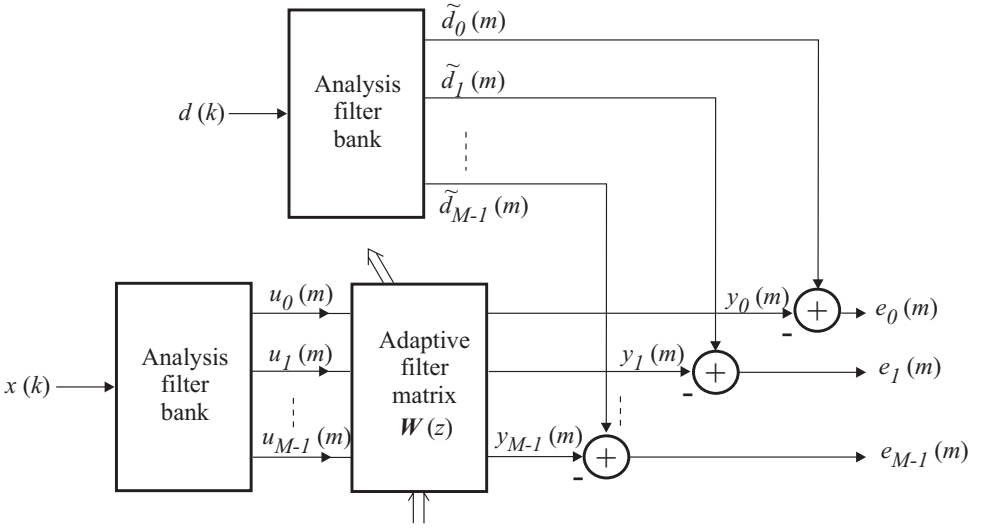

Figure 12.10 Open-loop subband structure.

For the open-loop structure, the objective function can be a linear combination of the magnitude square of the local errors as follows

$$\xi = \sum_{i=0}^{M-1} E[|e_i(m)|^2] \tag{12.22}$$

If we assume that the adaptive-filter matrix is diagonal, and that the subband signals are complex, the updating equation for the subband adaptive filters based on the normalized LMS algorithm is given by

$$e_i(m) = \tilde{d}_i(m) - \mathbf{w}_i^T(m)\mathbf{u}_i(m) \tag{12.23}$$

$$\mathbf{w}_i(m+1) = \mathbf{w}_i(m) + \frac{2\mu}{\gamma + N_s\sigma_i^2(m)} e_i(m)\mathbf{u}_i^*(m) \tag{12.24}$$

where N_s is the length of the adaptive filter in the ith subband (which we consider the same for all subbands in order to simplify the notation). In addition, $\sigma_i^2(m) = (1-\alpha)\sigma_i^2(m-1) + \alpha\,|u_i(m)|^2$, with α being a small factor chosen in the range $0 < \alpha \leq 0.1$, and γ is a small constant to prevent the updating factor from getting too large. The signal $e_i(m)$ is the subband error signal at the ith subband, and $\mathbf{u}_i(m)$ is the input signal vector to the ith adaptive filter.

Based on our knowledge of the normalized LMS algorithms, we can conjecture that the range of values for the convergence factor is typically[3]

$$0 < \mu < 1 \tag{12.25}$$

[3]The upper bound can be tighter depending on the input signal statistics.

Algorithm 12.1

Open-Loop Subband Adaptive-Filtering Algorithm

Initialization

$\mathbf{x}(0) = \mathbf{w}_l(0) = [0\,0\ldots0]^T$

$\gamma =$ small constant

$0 < \alpha \leq 0.1$

Do for each $x(iL)$ and $d(iL)$ given, for $i \geq 0$

$$\mathbf{u}(m) = \begin{bmatrix} u_0(m) \\ \vdots \\ u_{M-1}(m) \end{bmatrix} = \begin{bmatrix} \mathbf{E}_0 & \cdots & \mathbf{E}_{N_p} \end{bmatrix} \begin{bmatrix} \mathbf{x}(i) \\ \vdots \\ \mathbf{x}(i-N_p) \end{bmatrix}$$

$$\tilde{\mathbf{d}}(m) = \begin{bmatrix} \mathbf{E}_0 & \cdots & \mathbf{E}_{N_p} \end{bmatrix} \begin{bmatrix} \mathbf{d}(i) \\ \vdots \\ \mathbf{d}(i-N_p) \end{bmatrix}$$

$$\mathbf{y}(m) = \begin{bmatrix} y_0(m) \\ \vdots \\ y_{M-1}(m) \end{bmatrix} = \begin{bmatrix} \mathbf{W}_0 & \cdots & \mathbf{W}_{N_s} \end{bmatrix} \begin{bmatrix} \mathbf{u}(m) \\ \vdots \\ \mathbf{u}(m-N_s) \end{bmatrix}$$

$\mathbf{e}(m) = \tilde{\mathbf{d}}(m) - \mathbf{y}(m)$

Do for each for $0 \leq l \leq M-1$

$\sigma_l^2(m) = (1-\alpha)\sigma_l^2(m-1) + \alpha\,|u_l(m)|^2$

$\mathbf{w}_l(m+1) = \mathbf{w}_l(m) + \frac{2\mu}{\gamma + N_s\sigma_l^2(m)} e_l(m)\mathbf{u}_l^*(m)$

The steps of the open-loop algorithm are described in Algorithm 12.1, where $\mathbf{x}(iL-l)$ and $\mathbf{d}(iL-l)$ represent a block of the input and desired signals respectively, $\mathbf{E}_l$, for $l = 0, 1, \ldots, N_p$, are the matrices containing the coefficients of the polyphase representation of the analysis filter bank, that is,

$$\mathbf{E}(z) = \sum_{l=0}^{N_p} \mathbf{E}_l z^{-l}$$

The coefficient matrices $\mathbf{W}_l$, for $l = 0, 1, \ldots, N_s$, are the entries of the adaptive filter matrices.

Since the frequency responses of the subfilters that compose the filter bank are not ideal, the minimization of an objective function based on local errors will not necessarily reduce the fullband error energy to a minimum MSE. In this case, the unknown system might not be identified accurately.

12.4.1 Subband Identification

Define the $\mathcal{Z}$-transforms of the blocked versions of input and desired signals $x(k)$ and $d(k)$ as

$$\begin{aligned}\mathbf{X}(z) &= \sum_m \mathbf{x}(m)z^{-m} \\ \mathbf{D}(z) &= \sum_m \mathbf{d}(m)z^{-m}\end{aligned} \tag{12.26}$$

where $\mathbf{x}(m)$ is given in equation (12.6), and

$$\mathbf{d}(m) = [d(mL) \;\; d(mL-1)\ldots d(mL-L+1)]^T \tag{12.27}$$

If we describe the analysis filter transfer functions $F_i(z)$, for $i = 0, 1, \ldots, L-1$, in terms of their polyphase components, the subband input and desired signals, described in the $\mathcal{Z}$-domain for the critically decimated case (i.e. $L = M$), can be written in vector form as

$$\begin{aligned}\boldsymbol{\mathcal{Y}}(z) &= \mathbf{W}(z)\mathbf{E}(z)\mathbf{X}(z) \\ \boldsymbol{\mathcal{D}}(z) &= \mathbf{E}(z)\mathbf{D}(z)\end{aligned} \tag{12.28}$$

where $\boldsymbol{\mathcal{D}}(z)$ is the desired signal split into subbands, and $\boldsymbol{\mathcal{Y}}(z)$ is the adaptive system output (refer to Figs. 12.7 and 12.10).

By describing the unknown system model in the block form, as explained in subsection 12.3.6, the blocked desired signal is given by

$$\mathbf{D}(z) = \mathbf{H}(z)\mathbf{X}(z) \tag{12.29}$$

By substituting the above expression into equation (12.28), we obtain

$$\boldsymbol{\mathcal{D}}(z) = \mathbf{E}(z)\mathbf{H}(z)\mathbf{X}(z) \tag{12.30}$$

By defining the channel error vector as $\boldsymbol{\mathcal{E}}(z) = \boldsymbol{\mathcal{D}}(z) - \boldsymbol{\mathcal{Y}}(z)$ and setting it to zero, for $\mathbf{X}(z) \neq 0$, we generate the optimal solution for the adaptive-filter coefficient matrix

$$\mathbf{E}(z)\mathbf{H}(z) = \mathbf{W}_o(z)\mathbf{E}(z) \tag{12.31}$$

whose expression is given by

$$\mathbf{W}_o(z) = \mathbf{E}(z)\mathbf{H}(z)\mathbf{E}^{-1}(z) \tag{12.32}$$

Note that since $\mathbf{W}_o(z)$ is nondiagonal, it requires cross filters among channels in order to model the unknown system perfectly.

12.4.2 Two-Band Identification

The two-band case is easier to analyze in closed form, leading to interesting insights into the problem of cross filters. Using the relations described in equations (12.12) and (12.13), and considering the error signals equal to zero in Fig. 12.10, we can show that for the identification of an unknown transfer function $H(z)$, the optimal coefficients for the two-band adaptive filter are given by

$$\begin{aligned}\mathbf{W}_o(z) &= \begin{bmatrix} F_0(z^{\frac{1}{2}}) & F_0(-z^{\frac{1}{2}}) \\ F_1(z^{\frac{1}{2}}) & F_1(-z^{\frac{1}{2}}) \end{bmatrix} \begin{bmatrix} H(z^{\frac{1}{2}}) & 0 \\ 0 & H(-z^{\frac{1}{2}}) \end{bmatrix} \frac{1}{\Xi(z)} \begin{bmatrix} F_1(-z^{\frac{1}{2}}) & -F_0(-z^{\frac{1}{2}}) \\ -F_1(z^{\frac{1}{2}}) & F_0(z^{\frac{1}{2}}) \end{bmatrix} \\ &= \frac{1}{\Xi(z)} \begin{bmatrix} A(z) & -F_0(z^{\frac{1}{2}})F_0(-z^{\frac{1}{2}})[H(z^{\frac{1}{2}}) - H(-z^{\frac{1}{2}})] \\ F_1(z^{\frac{1}{2}})F_1(-z^{\frac{1}{2}})[H(z^{\frac{1}{2}}) - H(-z^{\frac{1}{2}})] & B(z) \end{bmatrix}\end{aligned} \tag{12.33}$$

where

$$\begin{aligned}\Xi(z) &= F_0(z^{\frac{1}{2}})F_1(-z^{\frac{1}{2}}) - F_0(-z^{\frac{1}{2}})F_1(z^{\frac{1}{2}}) \\ A(z) &= F_0(z^{\frac{1}{2}})F_0(-z^{\frac{1}{2}})H(z^{\frac{1}{2}}) - F_0(-z^{\frac{1}{2}})F_1(z^{\frac{1}{2}})H(-z^{\frac{1}{2}}) \\ B(z) &= -F_0(-z^{\frac{1}{2}})F_1(z^{\frac{1}{2}})H(z^{\frac{1}{2}}) + F_0(z^{\frac{1}{2}})F_1(-z^{\frac{1}{2}})H(-z^{\frac{1}{2}})\end{aligned}$$

The right-hand side of equation (12.33) shows that nonzero off-diagonal elements are required in order to model the unknown system. Note that the products of $F_0(z^{\frac{1}{2}})F_0(-z^{\frac{1}{2}})$ and $F_1(z^{\frac{1}{2}})F_1(-z^{\frac{1}{2}})$ would be null if the analysis filter bank were ideal. In the case of a nonideal filter bank, ill-conditioned signals appear in the adaptive part of the cross filters (which model the term $[H(z^{\frac{1}{2}}) - H(-z^{\frac{1}{2}})]$), leading to slow convergence of the adaptive cross filters.

12.4.3 Closed-Loop Structure

An alternative subband adaptive-filtering realization is the closed-loop structure depicted in Fig. 12.11. In the closed-loop structure, the fullband output signal of the adaptive filter is reconstructed through a synthesis filter bank, and the overall error signal is computed and utilized in the objective function. The overall error is split into subbands, which are then used in the adaptation algorithm. In the closed-loop scheme we aim to minimize the fullband error energy. In this case, the NLMS updating equation is given by

$$\mathbf{w}_i(m+1) = \mathbf{w}_i(m) + \frac{2\mu}{\gamma + N_s\sigma_i^2(m)}\mathbf{u}_i^*(m-\Delta)e_i'(m) \tag{12.34}$$

where the fullband error is evaluated as $e(k) = d(k - \Delta L) - y(k)$, and $e_i'(m)$ corresponds to the ith component of the fullband error signal split into subbands. The delay Δ is key to compensate for the extra delay the input signal faces, due to the analysis and synthesis filter bank, with respect to the desired signal. The delay value is given by

$$\Delta = \lfloor \frac{2KM - 1}{L} \rfloor \tag{12.35}$$

where $\lfloor(\cdot)\rfloor$ denotes the integer part of $(\cdot)$, $2KM$ is the length of the subfilters of the analysis and synthesis filter banks, and K is a positive integer number. The closed-loop scheme allows for the

Algorithm 12.2

Closed-Loop Subband Adaptive-Filtering Algorithm

Initialization

$\mathbf{x}(0) = \mathbf{w}_l(0) = [0\,0\,\ldots\,0]^T$

$\gamma =$ small constant

$0 < \alpha \leq 0.1$

Do for each $x(iL)$ and $d(iL)$ given, for $i \geq 0$

$$\mathbf{u}(m) = \begin{bmatrix} \mathbf{E}_0 & \cdots & \mathbf{E}_{N_p} \end{bmatrix} \begin{bmatrix} \mathbf{x}(i) \\ \vdots \\ \mathbf{x}(i-N_p) \end{bmatrix}$$

$$\mathbf{y}(m) = \begin{bmatrix} \mathbf{W}_0 & \cdots & \mathbf{W}_{N_s} \end{bmatrix} \begin{bmatrix} \mathbf{u}(m) \\ \vdots \\ \mathbf{u}(m-N_s) \end{bmatrix}$$

$$y(k) = \begin{bmatrix} 1 & \cdots & 1 \end{bmatrix} \begin{bmatrix} \mathbf{R}_0 & \cdots & \mathbf{R}_{N_p} \end{bmatrix} \begin{bmatrix} \mathbf{y}(m) \\ \vdots \\ \mathbf{y}(m-N_p) \end{bmatrix}$$

$$e(k) = d(k-\Delta L) - y(k)$$

$$\mathbf{e}'(m) = \begin{bmatrix} \mathbf{E}_0 & \cdots & \mathbf{E}_{N_p} \end{bmatrix} \begin{bmatrix} \mathbf{e}(i) \\ \vdots \\ \mathbf{e}(i-N_p) \end{bmatrix}$$

Do for each for $0 \leq l \leq M-1$

$\sigma_l^2(m) = (1-\alpha)\sigma_l^2(m-1) + \alpha\,|u_l(m)|^2$

$\mathbf{w}_l(m+1) = \mathbf{w}_l(m) + \frac{2\mu}{\gamma + N_s\sigma_l^2(m)}\mathbf{u}_l^*(m-\Delta)e_l'(m)$

minimization of a cost function based on the fullband error signal, and guarantees that the algorithm converges to a minimum MSE.

The closed-loop algorithm is described in detail in Algorithm 12.2. Note that the matrix coefficient $\mathbf{R}_l$, for $l = 0, 1, \ldots, N_p$, represents the element of order l of the synthesis filter polyphase matrix, and $\mathbf{y}(m-l)$ is the subband adaptive-filter output vector at time instant $(m-l)$. A comparison between the two schemes shows that the open-loop scheme generates an excess MSE because it actually minimizes the subband error energy, whereas the closed-loop scheme minimizes the fullband error. On the other hand, since in the closed-loop scheme a delay is introduced by the synthesis filter bank, and by the analysis filter bank applied to the error signal $e(k)$, the adaptation algorithm uses past information about the error signal, which can be shown to slow down the convergence. In fact, this delay reduces the upper bound of μ that can be employed in the closed-loop algorithm. The recursive

equations governing the convergence of the adaptive-filter coefficients of the closed-loop algorithm have the following general characteristics polynomial (see problem 8)

$$p(\Delta) = z^{\Delta+1} - z^{\Delta} + 2\mu\lambda_i = 0 \tag{12.36}$$

where Δ is the delay introduced by the filter banks and λ_i is related to the maximum eigenvalue of the autocorrelation matrix of the input signal in the ith subband. Considering the critical case of maximum eigenvalue $\lambda_{\max}$, the critical value of μ such that the zeros of equation (12.36) meet at the real axis is

$$\mu_{\text{crit}} = \frac{(\Delta-1)^{\Delta-1}}{2\lambda_{\max}\Delta^{\Delta}} \tag{12.37}$$

For higher values of μ the zeros move away from the real axis and eventually reach the unit circle at $\mu \approx 4.5\mu_{\text{crit}}$, see [17] and [16] for further details. Higher delays lead to lower values of μ. As a consequence, the closed-loop structures are more susceptible to convergence problems and less used in practice.

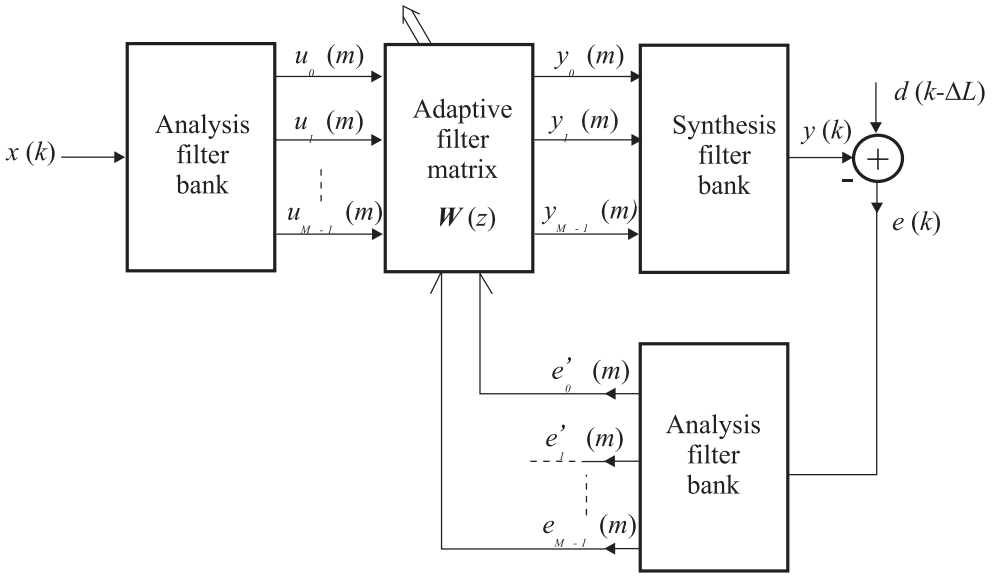

Figure 12.11 Closed-loop subband structure.

For the closed-loop structure, the excess MSE due to gradient noise (which tends to zero as $\mu \to 0$) is not related to the additional error resulting from the use of non-ideal filter banks. By making some simplifying assumptions, we can easily estimate the excess MSE in the closed-loop structure (the open-loop scheme follows similar analysis). The final result will closely follow the one for the standard LMS algorithm. If we consider that the input signal in each subband and the adaptive-filter coefficients are uncorrelated, and that the subfilters in the filter bank are frequency selective, we

can calculate the excess MSE individually in each subband, and combine them to derive the overall excess MSE. The result is given by

$$\xi_{exc} \approx \sum_{i=0}^{M-1} \frac{\mu_i \sigma_{n_i}^2 \mathrm{tr}[\mathbf{U}_i]}{1 - \mu_i \mathrm{tr}[\mathbf{U}_i]} \tag{12.38}$$

where $\mathbf{U}_i = E[\mathbf{u}_i(k)\mathbf{u}_i^H(k)]$, $\sigma_{n_i}^2 \approx \sigma_n^2/M$, and $\mu_i = \frac{\mu}{\gamma + N_s \sigma_i^2}$. This equation provides a good estimate to the excess MSE when the assumptions are closely met. A more accurate estimate is not straightforward to obtain.

Example 12.1

Identify an unknown system with the following transfer function

$$H(z) = \frac{0.1z}{(z + 0.9)} + \frac{0.08z}{(z^2 + 0.92)} + \frac{0.1z}{(z - 0.9)}$$

The input signal is a uniformly distributed white noise with variance $\sigma_x^2 = 1$, and the measurement noise is Gaussian white noise uncorrelated with the input with variance $\sigma_n^2 = 10^{-3}$. The filter bank is a cosine-modulated type of length 32.

(a) Start with a fullband filter using the normalized LMS algorithm.

(b) Compare the results obtained with those using an open-loop subband adaptive filter with three bands. Plot the MSE for an average of five independent runs, including the local errors and the overall error.

Solution:

Fig. 12.12 shows the MSE for the fullband normalized LMS algorithm.

The impulse response of the unknown system has infinite length. However, since the samples after 90 are rather small, we use three subband filters of length 30 each. No cross filters are employed. The convergence factor in all subbands is $\mu = 0.1$, and the parameters of the normalized updating equation are given by: $\alpha = 0.1$ and $\gamma = 0.001$. The prototype filter coefficients of the cosine-modulated filter bank are given in Table 12.1. Figs. 12.13 and 12.14 depict the MSE measured in the subbands and the global error computed after reconstruction of the adaptive-filter output through the synthesis filter bank. As can be observed, the convergence speed of global and local errors are not reduced due to the aliasing effects caused by the analysis filter banks. The aliasing errors appear at the global error and cannot be cancelled by the synthesis filter bank. As we can observe in Fig. 12.12, the fullband normalized LMS algorithm achieves a larger reduction in the excess of MSE since in this case there are no aliasing effects. In both examples, some excess MSE is expected since the unknown system has infinite length.

□

Table 12.1 Coefficients of the prototype filter of the cosine modulated filter bank

n	$f(n)$	n	$f(n)$	n	$f(n)$	n	$f(n)$
0	0.000689	8	-0.023394	16	0.188567	24	-0.015614
1	-0.000316	9	-0.023179	17	0.163319	25	-0.005030
2	0.001608	10	-0.008268	18	0.119646	26	0.001726
3	0.003180	11	0.023394	19	0.069041	27	0.004631
4	0.004631	12	0.069041	20	0.023394	28	0.003180
5	0.001726	13	0.119646	21	-0.008268	29	0.001608
6	-0.005030	14	0.163319	22	-0.023179	30	-0.000316
7	-0.015614	15	0.188567	23	-0.023394	31	0.000689

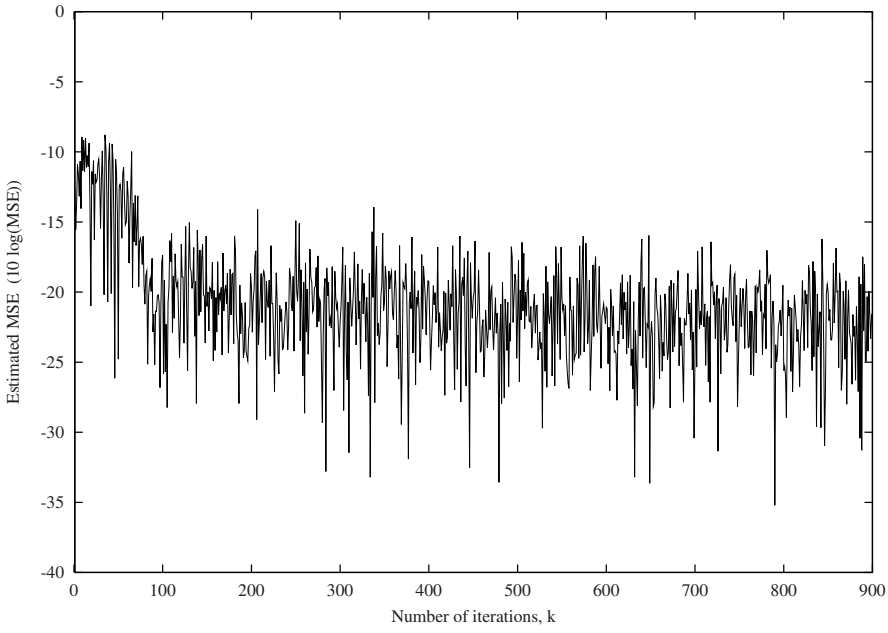

Figure 12.12 MSE in the fullband normalized LMS algorithm.

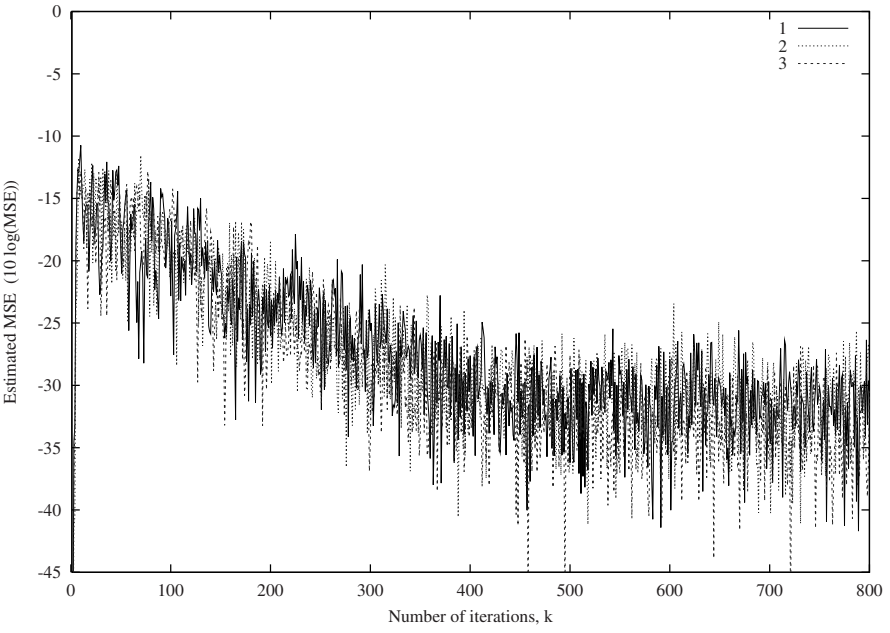

Figure 12.13 Subband errors in the open-loop structure.

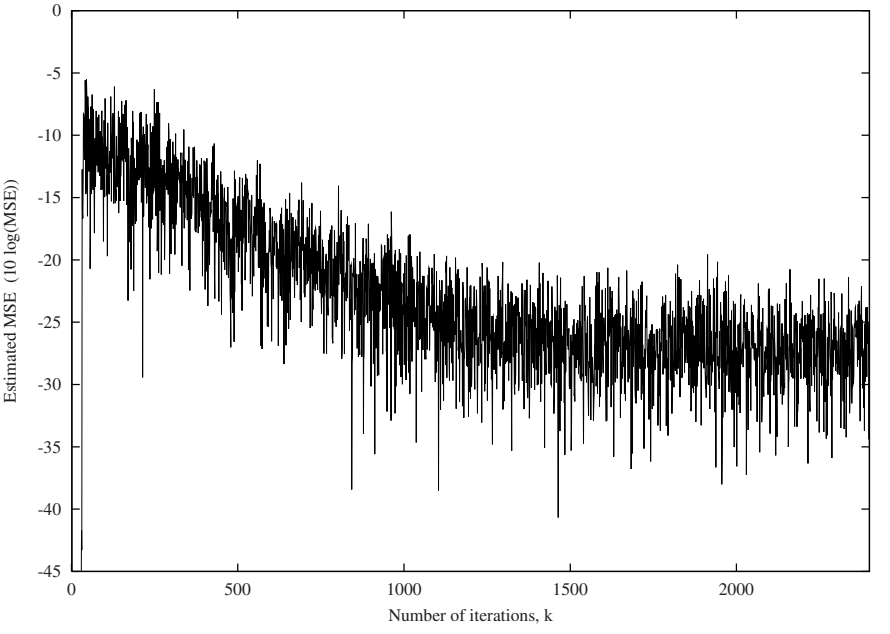

Figure 12.14 Global errors in the open-loop structure.

12.5 CROSS-FILTERS ELIMINATION

The design of sophisticated filter banks is beyond the scope of this book. Highly selective subfilters are key to reduce the importance of the cross filters, and eventually eliminate them. However, for moderately selective subfilters their elimination will always lead to an excess MSE at the adaptive-filter output. In this section, we discuss the design of a special type of maximally decimated ($M = L$) analysis filter bank for cross-filter elimination [23]. It will be verified that the generation of these filter banks requires the design of fractional delays, which will also be briefly discussed. The price paid for the elimination of the cross filters is the design of accurate fractional delays. Unlike the adaptive cross filters, the fractional delays are fixed filters.

A solution to avoid the cross filters in a maximally decimated structure can be engineered if we explore the special structure of the blocked matrix representation of the unknown system. This implementation is given in Fig. 12.7 with $\mathbf{H}(z)$ replacing the cascade of $\mathbf{E}(z)$ and $\mathbf{R}(z)$. In a subband adaptive-filtering configuration, this blocked matrix $\mathbf{H}(z)$ is followed by a parallel-to-serial converter, belonging to the unknown system, which in turn is in cascade with a serial-to-parallel converter, belonging to the analysis filter bank represented in the polyphase form. The cascade of these converters is an identity matrix multiplied by a delay as depicted in Fig. 12.15. Without loss of generality we can disregard the delay[4]. Since the polyphase matrix of the analysis filter bank $\mathbf{E}(z)$ follows the pseudocirculant matrix $\mathbf{H}(z)$, if we choose an $\mathbf{E}(z)$ as a similarity transformation matrix which transforms $\mathbf{H}(z)$ into its Jordan form, we can avoid most of (usually all) the off-diagonal elements of the adaptive-filter matrix $\mathbf{W}(z)$. As mentioned in [18], the Jordan form is the extreme effort in diagonalizing a matrix. The full diagonalization is impossible only for defective matrices.

In the following discussions, we assume that $\mathbf{H}(z)$ is not defective and therefore diagonalizable, that is, there is a $\mathbf{T}(z)$ such that

$$\mathbf{T}(z)\mathbf{H}(z)\mathbf{T}^{-1}(z) = \begin{bmatrix} \mathcal{W}_{o,0}(z) & 0 & \cdots & 0 \\ 0 & \mathcal{W}_{o,1}(z) & \cdots & 0 \\ \vdots & \vdots & \ddots & \vdots \\ 0 & 0 & \cdots & \mathcal{W}_{o,L-1}(z) \end{bmatrix} \tag{12.39}$$

The matrix $\mathbf{T}^{-1}(z)$, whose columns are the eigenvectors of any $L \times L$ pseudocirculant matrix, is given by[5]

$$\mathbf{T}^{-1}(z) = \mathbf{\Gamma}(z)\mathcal{F} \tag{12.40}$$

[4]This delay would not appear if we had employed a noncausal representation for the parallel-to-serial converter.

[5]In fact, any pseudocirculant matrix $\mathbf{H}(z)$ can be written as $\mathbf{\Gamma}(z)\mathbf{H}_c(z)\mathbf{\Gamma}^{-1}(z)$ where $\mathbf{H}_c(z)$ is a circulant matrix. Since any circulant matrix is diagonalized as $\mathcal{F}^*\mathbf{H}_c(z)\mathcal{F}$, with $\mathcal{F}^*$ being the inverse of $\mathcal{F}$ (in this case just the complex conjugate), the result of equation (12.40) follows.

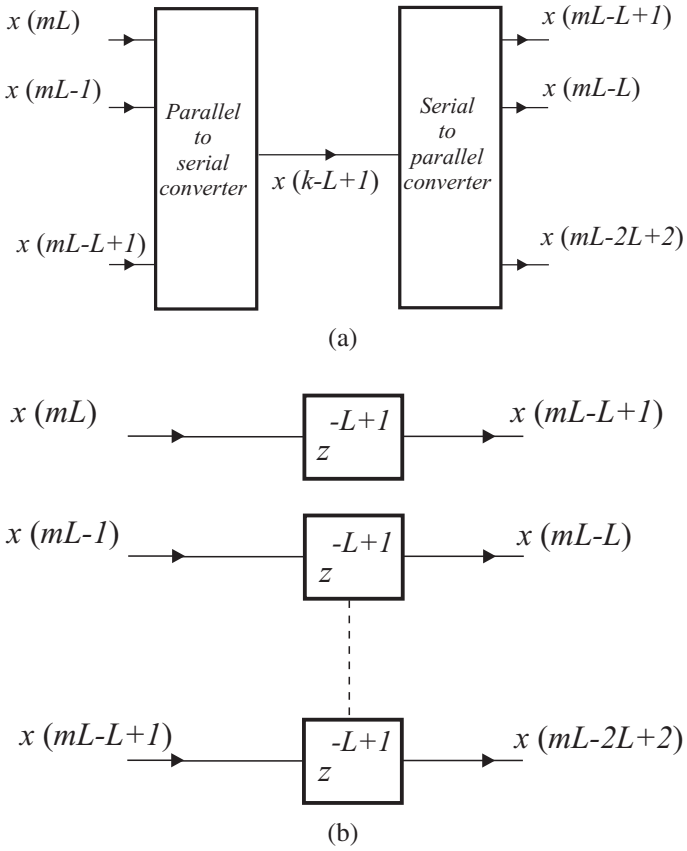

Figure 12.15 (a) Cascade connection of block converters, (b) Equivalent circuit.

where $\mathcal{F}$ is the $L \times L$ DFT matrix whose element (i, j), for $i, j = 0, 1, \ldots, L-1$, is given by $\frac{W^{ij}}{\sqrt{L}}$, where $W = \mathrm{e}^{\frac{-j2\pi}{L}}$, and

$$\mathbf{\Gamma}(z) = \begin{bmatrix} 1 & 0 & \cdots & 0 \\ 0 & z^{-\frac{1}{L}} & \cdots & 0 \\ \vdots & \vdots & \ddots & \vdots \\ 0 & 0 & \cdots & z^{-\frac{L-1}{L}} \end{bmatrix} \tag{12.41}$$

Now if we examine equations (12.32) and (12.39) more closely, we conclude that by choosing the polyphase matrix as $\mathbf{E}(z) = \mathbf{T}(z)z^{-\frac{L-1}{L}}$, where the delay was included in order to guarantee causality of the analysis filter bank, the cross filters are eliminated.

The optimal adaptive subfilters are given by the eigenvalues of $\mathbf{H}(z)$ (refer to equation (12.39)), whose expressions are

$$\mathcal{W}_{o,i}(z) = \frac{1}{\sqrt{L}} \sum_{l=0}^{L-1} H_l(z) z^{-\frac{l}{L}} W^{li} \tag{12.42}$$

for $i = 0, 1, \ldots, M-1$, where $H_l(z)$ is the lth polyphase component of $H(z)$.

In conclusion, the polyphase-component matrix of the analysis filter bank is given by

$$\begin{aligned} \mathbf{E}(z) &= \mathcal{F}^* \mathbf{\Gamma}^{-1}(z) z^{-\frac{L-1}{L}} \\ &= \mathcal{F}^* \begin{bmatrix} z^{-\frac{L-1}{L}} & 0 & \cdots & 0 \\ 0 & z^{-\frac{L-2}{L}} & \cdots & 0 \\ \vdots & \vdots & \ddots & \vdots \\ 0 & 0 & \cdots & 1 \end{bmatrix} \end{aligned} \tag{12.43}$$

The structure of the analysis filter bank based on fractional delays is depicted in Fig. 12.16. Similarly, we can derive the structure for the synthesis filter bank utilizing fractional delays illustrated in Fig. 12.17. It is worth mentioning that selectivity of the subfilters in this type of bank is highly dependent on the quality of the fractional delays design. The filter banks based on fractional delays are particularly useful in the delayless subband structures of section 12.6.

12.5.1 Fractional Delays

The review article about fractional delays [31] proposes several techniques for the approximation of a fractional delay. One of them consists of designing a symmetric Lth band filter (also known as a Nyquist filter), and keeping its lth polyphase component to represent the fractional delay $\tilde{\Delta} + l/L$. The delay $\tilde{\Delta}$ is the integer part of the group delay inherent to the FIR filter approximating a fractional delay. The Lth band filter has an impulse response that satisfies

$$h(kL) = \begin{cases} K, & k = 0 \\ 0, & \text{otherwise} \end{cases} \tag{12.44}$$

where K is a constant value. In the $\mathcal{Z}$-domain, the representation of $h(k)$ is

$$H(z) = K + z^{-1} E_1(z^L) + \cdots + z^{-(L-1)} E_{L-1}(z^L) \tag{12.45}$$

If $H(z)$ satisfies the above condition, it can be shown that [9]

$$\sum_{l=0}^{L-1} H(zW^l) = LK \tag{12.46}$$

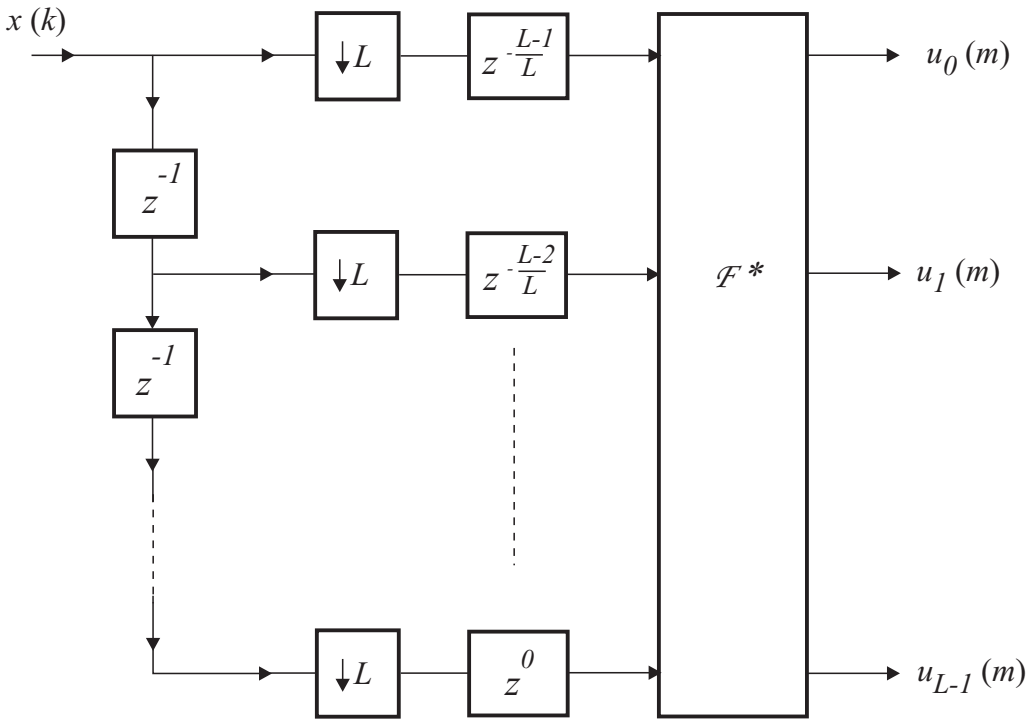

Figure 12.16 Analysis filter bank based on fractional delays.

where $W = \mathrm{e}^{-\frac{j2\pi}{L}}$. The proof for the above relation is straightforward, if we just replace z by zW^l in equation (12.45), and compute the summation in equation (12.46).

Therefore, a natural proposition to eliminate adaptive cross filters is to design a DFT filter bank with a lowpass prototype filter given by an Lth band filter whose polyphase components approximate the fractional delays. The Lth band filter can be easily designed by using the so called eigenfilter approach for FIR filter approximation [9]. This approach allows the incorporation of the constraints inherent in the Nyquist filters. The Lth band filter is usually designed as a lowpass filter whose passband (ω_p) and stopband (ω_s) edges are symmetric with respect to the normalized frequency $\frac{\pi}{L}$, that is $\omega_p + \omega_s = 2\frac{\pi}{L}$. Although the fractional delays designed using Lth band filters are not very accurate, they can be considered acceptable for the delayless structures discussed in section 12.6.

Another simple FIR filter design to approximate the fractional delay is through the classical Lagrange interpolation formula. The interested reader should refer to [31].

Example 12.2

Repeat example 12.1 with a filter bank using fractional delays.

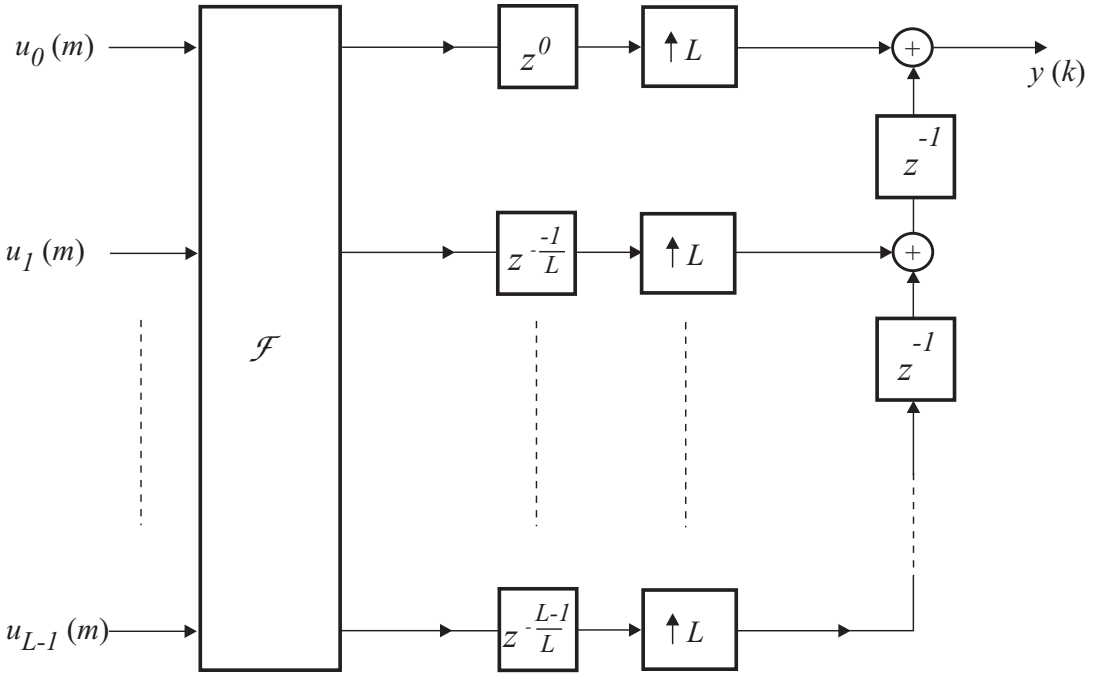

Figure 12.17 Synthesis filter bank based on fractional delays.

Solution:

For this example we design the fractional delays via a three-band filter. The length of the polyphase components is 9, with values given in Table 12.5.1. The length of the adaptive filters in the subbands is $N = 30$, the convergence factor in all subbands is $\mu = 0.1$, and parameters of the normalized updating equation are given by $\alpha = 0.1$ and $\gamma = 0.001$.

As can be observed in Figs. 12.18 and 12.19, the errors measured in the subbands and the global error are rather high due to the aliasing effects. Due to these effects, we can see in Fig. 12.20 that the magnitude response obtained after convergence resembles the unknown system response although the approximation is not very close.

□

Table 12.2 Coefficients of the fractional delays of the analysis filter bank

n	E_0	E_1	E_2
0	0.0000	0.0000	0.0000
1	-0.0072	-0.0117	0.0000
2	0.0320	0.0497	0.0000
3	-0.1090	-0.1592	0.0000
4	0.3880	0.8140	1.0000
5	0.8140	0.3880	0.0000
6	-0.1592	-0.1090	0.0000
7	0.0497	0.0320	0.0000
8	-0.0117	-0.0072	0.0000

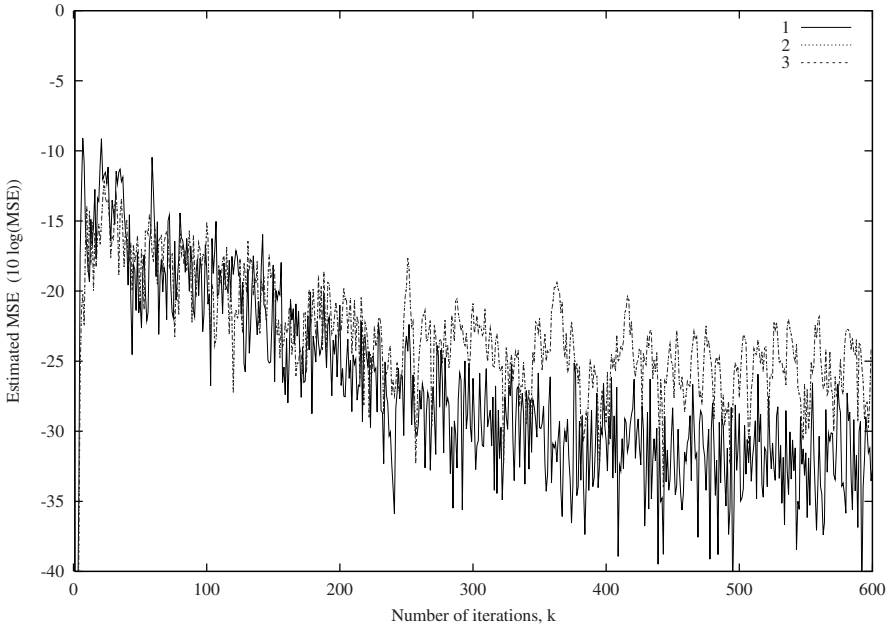

Figure 12.18 Subband errors in the open-loop structure.

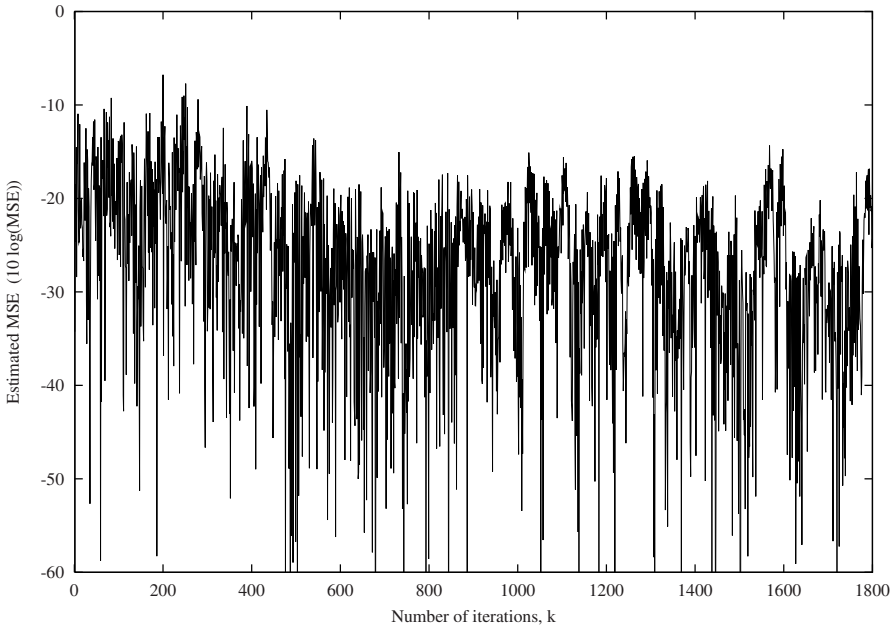

Figure 12.19 Global error in the open-loop structure.

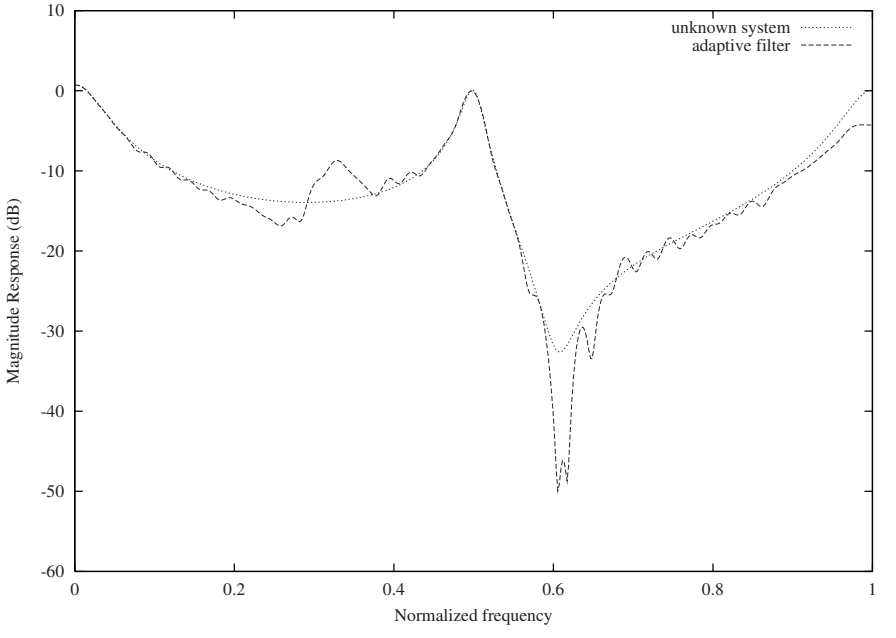

Figure 12.20 Magnitude responses of the unknown system and the obtained model at a given iteration.

12.6 DELAYLESS SUBBAND ADAPTIVE FILTERING

In the subband adaptive-filtering schemes presented so far, a delay is always introduced in the signal path due to the filter bank analysis and synthesis. In applications such as acoustic echo cancellation and active noise control, the delay is highly undesirable. In acoustic echo cancellation, the echo is not fully canceled and can be perceptually unacceptable. In active noise control the delay reduces the cancellation bandwidth [21].

In order to avoid the effect of signal path delay in these applications, we can avoid the synthesis filter bank and map the subband adaptive filters into a wideband filter, leading to the so called *delayless subband adaptive filters*. Several techniques to perform this mapping have been proposed [22]-[27], where the distinctive feature among them is the construction of each analysis filter bank and its corresponding subband to fullband mapping. In this section, we describe the delayless subband adaptive filter proposed in [23] which utilizes DFT-based filter banks with fractional delays discussed in this chapter. Fig. 12.21 depicts the general configuration of a delayless adaptive filter in subbands, employing a maximally decimated filter bank.

Equation (12.42) gives the coefficients of the optimal subband adaptive filters in each subband, for the open-loop scheme. The transfer functions of these subfilters represent the eigenvalues of a pseudocirculant matrix. Therefore, if we apply the inverse DFT to a vector whose elements are the transfer functions of the adaptive subfilters, we can recover the polyphase components estimates of the unknown system multiplied by fractional delays as described in the equation below

$$\frac{1}{\sqrt{L}}\begin{bmatrix} \hat{H}_0(z) \\ \hat{H}_1(z)z^{-\frac{1}{L}} \\ \vdots \\ \hat{H}_{L-1}(z)z^{-\frac{(L-1)}{L}} \end{bmatrix} = \mathcal{F}^*\left(\begin{bmatrix} \mathcal{W}_0(z) \\ \mathcal{W}_1(z) \\ \vdots \\ \mathcal{W}_{L-1}(z) \end{bmatrix}\right) \tag{12.47}$$

It should be noticed that in most cases the length of the adaptive subfilters is chosen as $\frac{N}{L}$, where N is the unknown system length. However, from the above equation some extra coefficient should be allotted to the subband adaptive filters in order to account for the fractional delays.

Since in our case any subfilter of the bank $F_i(z)$ has an inherent fractional delay, it is reasonable to conjecture that the product $F_i(z)z^{-\frac{i}{L}}$ represents a filter with one more sample than $F_i(z)$. Through a number of simulations, we concluded that a single coefficient is enough to perform this task in closed-loop schemes. As a consequence, the adaptive subfilters have length $N_s = \frac{N}{L} + 1$.

By denoting each element of the time-domain representation of $\mathcal{W}_i(z)$ as $w_{i,l}$, we can compute the previous equation in parts as follows

$$\begin{bmatrix} w'_{0,l} \\ w'_{1,l} \\ \vdots \\ w'_{L-1,l} \end{bmatrix} = \mathcal{F}^*\left(\begin{bmatrix} w_{0,l} \\ w_{1,l} \\ \vdots \\ w_{L-1,l} \end{bmatrix}\right) \tag{12.48}$$

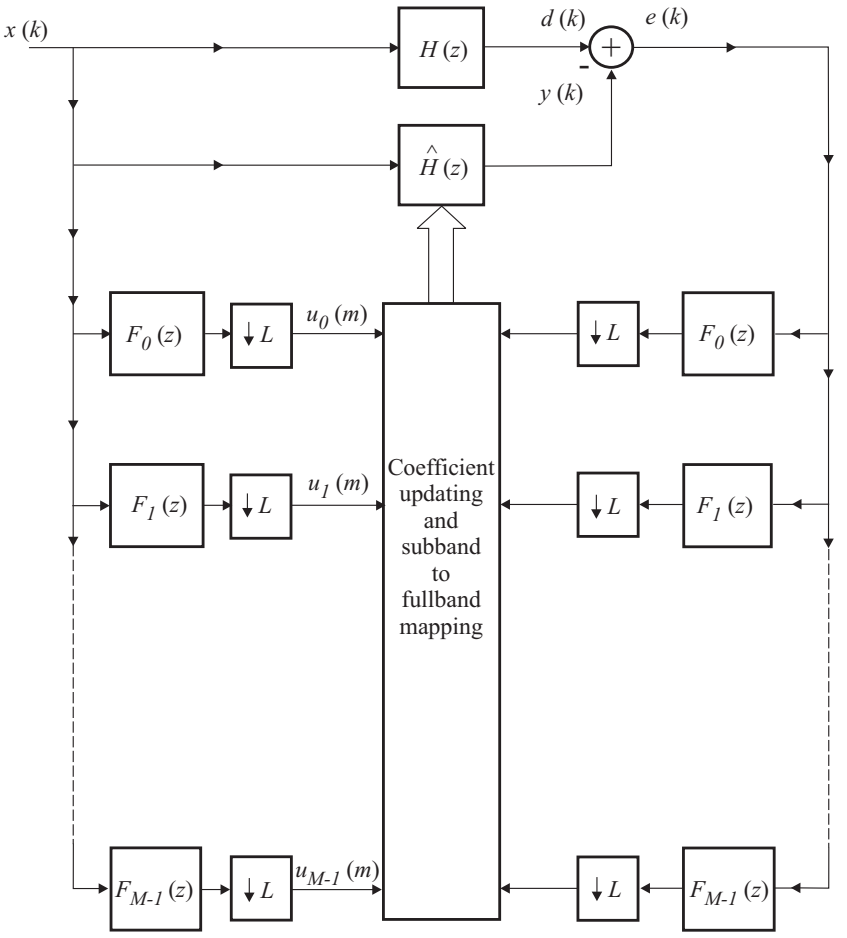

Figure 12.21 Delayless closed-loop subband structure.

for $l = 0, 1, \ldots, N_s - 1$. The polyphase component of the corresponding fullband adaptive filter is then given by $\frac{1}{\sqrt{L}} \hat{H}_i(z) z^{-\frac{i}{L}} = W_i'(z)$, where $W_i'(z)$ represents the $\mathcal{Z}$-transform of $w_{i,l}'$, and $\hat{H}_i(z)$ represents an estimate of the ith polyphase component of the unknown system. We can obtain the polyphase components $\hat{H}_i(z)$ from $W_i'(z)$, if we note that

$$\hat{H}_i(z) z^{-\frac{i}{L}} z^{-\frac{L-i}{L}} = \hat{H}_i(z) z^{-1} \tag{12.49}$$

for $i = 0, 1, \ldots, L-1$. The above discussion indicates that the cascade of $W_i'(z)$ with the fractional delay $E_{i-1}(z)$, $i = 1, \ldots, L-1$, leads to the polyphase component $\hat{H}_i(z)$ delayed by $\tilde{\Delta} + 1$ samples and scaled by $\frac{1}{\sqrt{L}}$. Recall that $\tilde{\Delta}$ is the integer part of the group delay introduced by the design of the fractional delays.

Note that the impulse response of $\hat{H}_0(z)$ is represented by $w'_{0,l}$. Similarly, we can infer that

$$\begin{aligned} \mathcal{W}'_0(z) &\approx \frac{1}{\sqrt{L}}\hat{H}_0(z) \\ \mathcal{W}'_i(z)E_{i-1}(z) &\approx \frac{1}{\sqrt{L}}\hat{H}_i(z)z^{-(\tilde{\Delta}+1)} \end{aligned} \tag{12.50}$$

for $i = 1, \ldots, M-1$. In conclusion, to obtain the first polyphase filter $\hat{H}_0(z)$ we simply discard the last sample of $w'_{0,l}$. For $\hat{H}_i(z)$, with $i = 1, \ldots, M-1$, we discard the first $\tilde{\Delta}+1$ samples and retain the next $N_s - 1$ samples (here the reader should recall that we used an extra coefficient for the adaptive subfilters to compensate for the fractional delay in the subfilter of the analysis bank). The fullband filter is then formed by

$$\hat{H}(z) = \sum_{i=0}^{L-1} \hat{H}_i(z^L)z^{-i} \tag{12.51}$$

The delayless closed-loop algorithm is described in detail in Algorithm 12.3, where $\mathbf{e}(mL)$ represents a length L block of the error signal at instant mL. The detailed structure is shown in Fig. 12.22. It is worth mentioning that the delayless closed-loop structure does not suffer as much from the stability problems inherent in the standard closed-loop subband structure. This is because we do not have to reconstruct the adaptive-filter output through a synthesis filter bank in order to generate the global error. This reconstruction originates part of the convergence problems of the standard closed-loop structure.

Example 12.3

Repeat example 12.1 using the closed-loop delayless structure whose filter banks employ fractional delays.

Solution:

For this example, we use the same parameters as Example 12.2. As can be observed in Figs. 12.23 and 12.24, the errors measured in the subbands and the global error are reduced despite the fact that the subfilters of the filter bank are not very selective. In this case, the delayless closed-loop structure is able to compensate for the limitations of the filter bank. Fig. 12.25 shows that the magnitude response obtained after convergence is very close to the unknown system response.

□

12.6.1 Computational Complexity

An interesting issue to illustrate the results of this chapter is to assess the overall computational complexity of the subband structure. The computational complexity is counted in multiplications

per input sample, and considering that the product of complex values is implemented through four real multiplications. In the delayless subband structure, the overall computation consists of the components described below.

- The subband decomposition: It consists of one convolution of an N_{pr}-length prototype filters, which is the total number of coefficients required to realize all the fractional delays, and one L-point FFT for each block of L input samples. Assuming that the number of complex

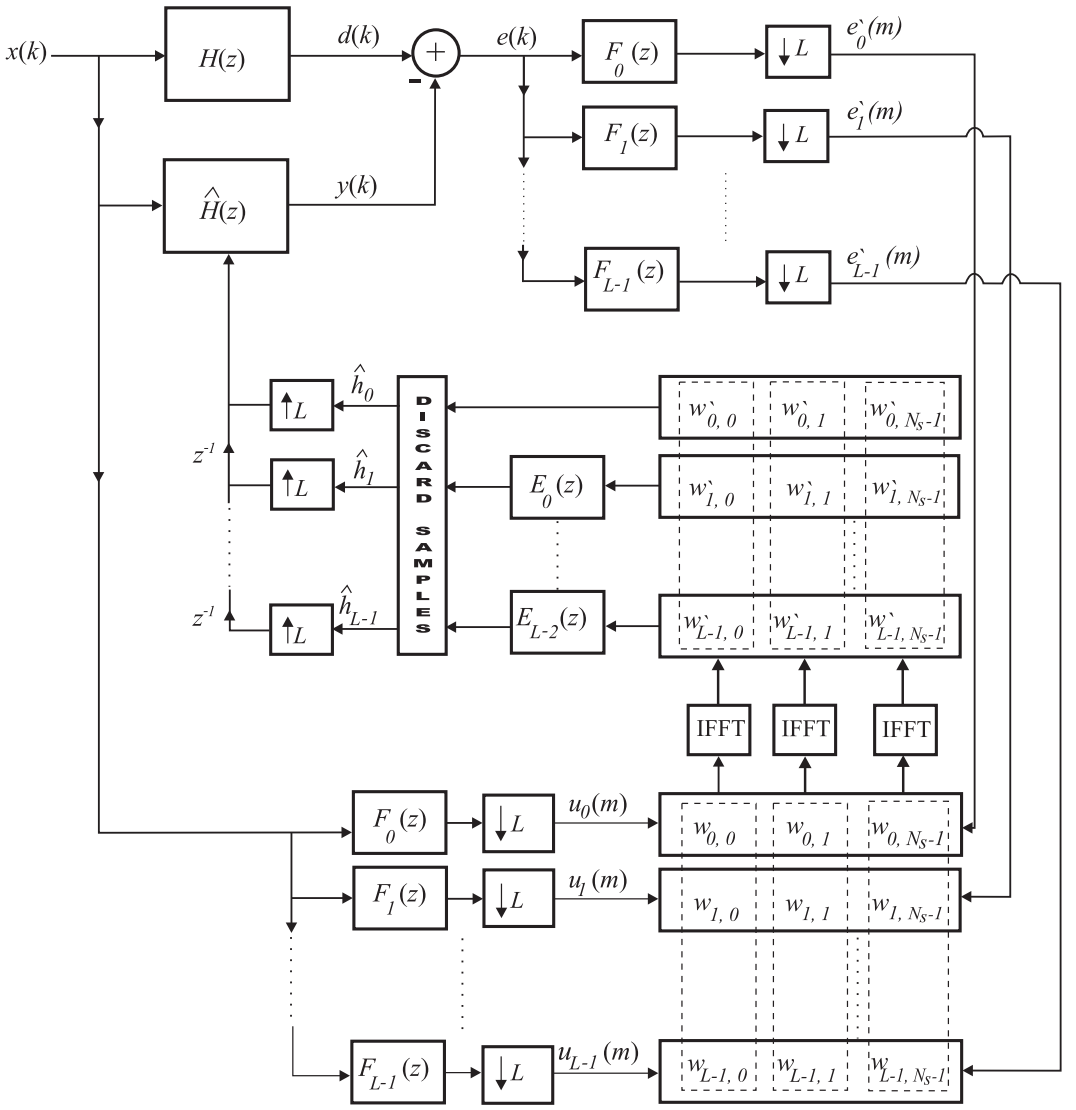

Figure 12.22 Detailed delayless closed-loop subband structure.

Algorithm 12.3

Delayless Closed-Loop Subband Adaptive-Filtering Algorithm

Initialization

$\mathbf{x}(0) = \mathbf{w}_l(0) = [0\,0\ldots0]^T$

$\gamma =$ small constant

$0 < \alpha \leq 0.1$

Do for each $x(iL)$ and $d(iL)$ given, for $i \geq 0$

$$\mathbf{u}(m) = \mathcal{F}^* \left[\begin{array}{cccc} \mathbf{E}_0 & \cdots & \mathbf{E}_{N_p} \end{array} \right] \left[\begin{array}{cccc} \mathbf{x}(i) & \cdots & \mathbf{x}(i-N_p) \end{array} \right]^T$$

where $\mathbf{E}_l$, for $l = 0, 1, \ldots, N_p$ are diagonal matrices whose elements are the lth element of the impulse response of the filter implementing the fractional delays, and N_p is the order of fractional delays implementation.

$$\begin{bmatrix} w'_{0,l} \\ w'_{1,l} \\ \vdots \\ w'_{L-1,l} \end{bmatrix} = \mathcal{F}^* \left(\begin{bmatrix} w_{0,l} \\ w_{1,l} \\ \vdots \\ w_{L-1,l} \end{bmatrix} \right)$$

Get $\frac{1}{\sqrt{L}}\hat{H}_0(z)$ by discarding the last sample of $w'_{0,l}$.

For $\frac{1}{\sqrt{L}}\hat{H}_i(z)$, with $i = 1, \ldots, L-1$, we discard the first $\tilde{\Delta}+1$ samples of the impulse response corresponding to equation (12.50) and retain the following $N_s - 1$ samples.

$\hat{\mathbf{h}}(k)$ is the impulse response of $\hat{H}(z) = \sum_{i=0}^{L-1} \hat{H}_i(z^L)z^{-i}$.

$e(k) = d(k) - \hat{\mathbf{h}}^H(k)\mathbf{x}(k)$

$$\mathbf{e}'(m) = \mathcal{F}^* \left[\begin{array}{cccc} \mathbf{E}_0 & \cdots & \mathbf{E}_{N_p} \end{array} \right] \left[\begin{array}{cccc} \mathbf{e}(i) & \cdots & \mathbf{e}(i-N_p) \end{array} \right]^T$$

Do for each for $0 \leq l \leq L-1$

$\sigma_l^2(m) = (1-\alpha)\sigma_l^2(m-1) + \alpha\,|u_l(m)|^2$

$\mathbf{w}_l(m+1) = \mathbf{w}_l(m) + \frac{2\mu}{\gamma + N_s\sigma_l^2(m)}\mathbf{u}_l^*(m)e'_l(m)$

multiplications required to compute a L-point FFT is $\frac{L}{2}\log_2 L$, see [33], we obtain

$$\frac{2N_{pr}}{L} + 2\log_2 L \tag{12.52}$$

real multiplications per input sample for the two analysis filter banks. The symmetry of the IDFT for real signals allows us to process only half of the L channel complex signals. Therefore, we have to update $\frac{L}{2}$ adaptive filters.

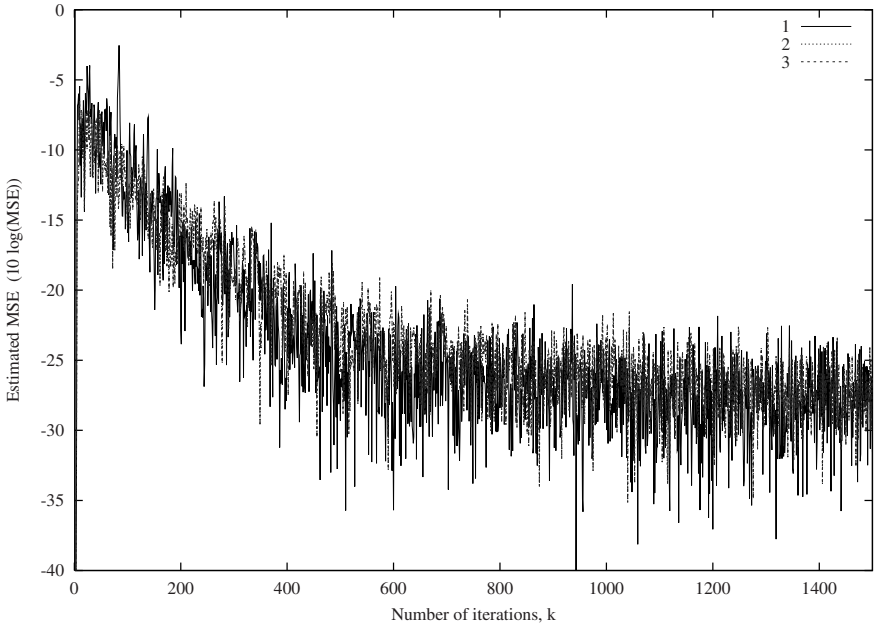

Figure 12.23 Subband errors in the closed-loop structure.

- The subband NLMS algorithm: Considering that we have to update $\frac{L}{2}$ adaptive filters of length $N_s = \frac{N}{L} + 1$ for every L input samples, the computational complexity entails

$$2\frac{N+L}{L} \tag{12.53}$$

real multiplications per input sample.

For the open-loop scheme an additional of $2\frac{N+L}{L}$ is required to evaluate the adaptive-filters outputs $y(m)$.

- The wideband filter convolution: There are some approaches to reduce the computational complexity of the wideband convolution as discussed in [22]. Here we consider only the direct implementation which entails N multiplications per output sample.

- The transformation from the subband adaptive filters to the wideband adaptive filter: It consists of N_s IFFTs and $L-1$ convolutions with the polyphase filters as indicated in equation (12.50). However, there is no need to perform the transformation for every L input samples, since in most applications the fullband adaptive-filter output cannot vary much faster then the length of filter impulse response. The computational cost is then given by

$$\frac{1}{r}\left[(\frac{N}{L}+1)\log_2 L + \frac{NN_{pr}(L-1)}{L^3}\right] \tag{12.54}$$

real multiplications per input sample, where rL represents how often the transformation is performed in terms of the number of input samples.

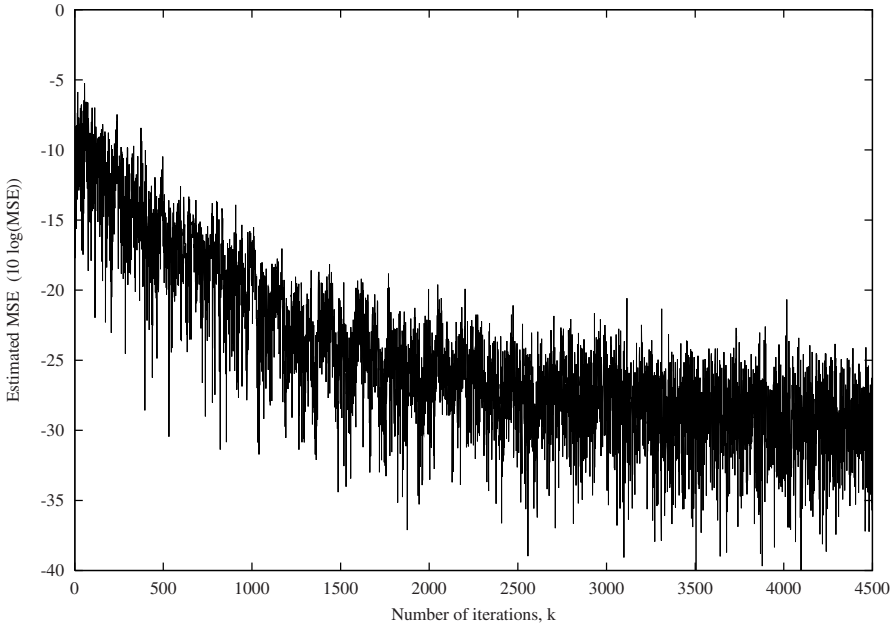

Figure 12.24 Global error in the closed-loop structure.

The overall computational complexity for the closed-loop scheme is

$$P_c = \frac{2N_{pr}}{L} + 2\log_2 L + \frac{2(N+L)}{L} + \frac{1}{r}\left[(\frac{N}{L}+1)\log_2 L + \frac{NN_{pr}(L-1)}{L^3}\right] + N \quad (12.55)$$

while for the open-loop scheme we have

$$P_o = \frac{2N_{pr}}{L} + 2\log_2 L + \frac{4(N+L)}{L} + \frac{1}{r}\left[(\frac{N}{L}+1)\log_2 L + \frac{NN_{pr}(L-1)}{L^3}\right] + N \quad (12.56)$$

12.7 FREQUENCY-DOMAIN ADAPTIVE FILTERING

Frequency-domain adaptive algorithms, which employ block processing in order to reduce the computational complexity associated with high-order adaptive filters, have been suggested in [34]. Such algorithms utilize FFTs to implement convolutions (for filtering) and correlations (for coefficient updating). More general block algorithms, in which the block size can be smaller than the order of the adaptive filter, have also been investigated [35]. Such approach, called *multidelay adaptive filter* (MDF) [37]-[40], utilizes adaptive filters in the bins (equivalent to the subbands), unlike the original frequency-domain adaptive-filtering algorithms that use a single adaptive coefficient in each bin. Like the subband adaptive filters discussed so far, frequency-domain adaptive filters can increase the convergence speed by decreasing the eigenvalue spread of the autocorrelation matrices of the signals

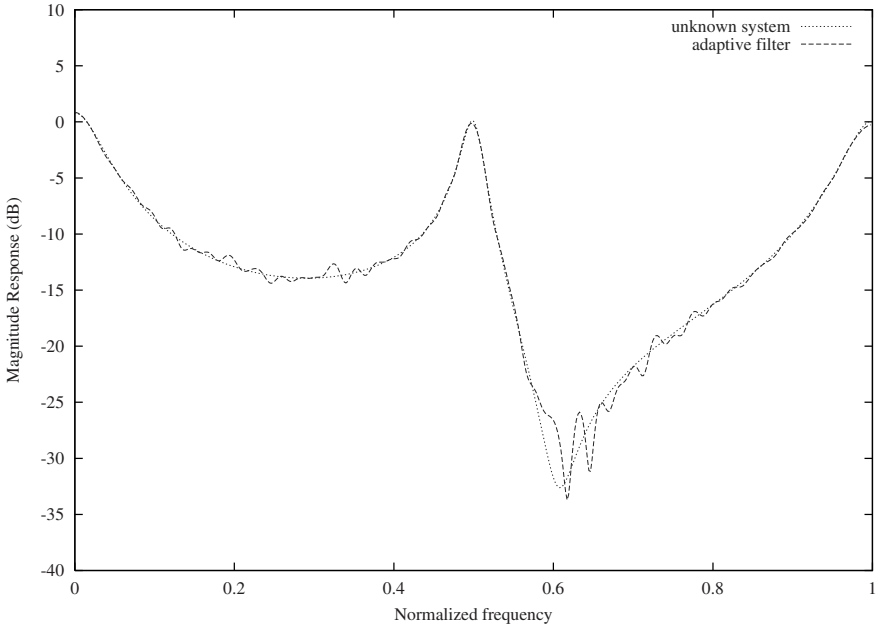

Figure 12.25 Magnitude responses of the unknown system and the obtained model at a given iteration.

at the inputs of the adaptive filters. In fact, the subband and the frequency-domain adaptive filters are closely related as will become clear in the sequel.

Let us consider the case where both the input and desired signals are presented in their corresponding blocked versions as described in subsection 12.3.6. The adaptive filter transfer function is represented by a blocked matrix denoted by $\hat{\mathbf{H}}(z)$. In this case, the adaptive-filter output is also represented in block form $\mathbf{y}(m)$, which in turn is compared with the desired signal block $\mathbf{d}(m)$. These vectors are defined as

$$\begin{aligned}\mathbf{y}(m) &= [y(mL)\, y(mL-1) \ldots y(mL-L+1)]^T \\ \mathbf{x}(m) &= [x(mL)\, x(mL-1) \ldots x(mL-L+1)]^T \\ \mathbf{d}(m) &= [d(mL)\, d(mL-1) \ldots d(mL-L+1)]^T \end{aligned} \tag{12.57}$$

In the particular case where the matrix $\hat{\mathbf{H}}(z)$ is 3×3, we have

$$\begin{aligned}\hat{\mathbf{H}}(z) &= \begin{bmatrix} \hat{H}_0(z) & \hat{H}_1(z) & \hat{H}_2(z) \\ z^{-1}\hat{H}_2(z) & \hat{H}_0(z) & \hat{H}_1(z) \\ z^{-1}\hat{H}_1(z) & z^{-1}\hat{H}_2(z) & \hat{H}_0(z) \end{bmatrix} \\ &= \hat{\mathbf{H}}_0(z)\hat{\mathbf{H}}_1(z) \end{aligned} \tag{12.58}$$

where $\hat{H}_i(z)$, $i = 0, 1, 2$, are the polyphase components of $W(z)$, and

$$\hat{\mathbf{H}}_0(z) = \begin{bmatrix} \hat{H}_0(z) & \hat{H}_1(z) & \hat{H}_2(z) & 0 & 0 & 0 \\ 0 & \hat{H}_0(z) & \hat{H}_1(z) & \hat{H}_2(z) & 0 & 0 \\ 0 & 0 & \hat{H}_0(z) & \hat{H}_1(z) & \hat{H}_2(z) & 0 \end{bmatrix}$$

$$\hat{\mathbf{H}}_1(z) = \begin{bmatrix} 1 & 0 & 0 \\ 0 & 1 & 0 \\ 0 & 0 & 1 \\ z^{-1} & 0 & 0 \\ 0 & z^{-1} & 0 \\ 0 & 0 & z^{-1} \end{bmatrix} \tag{12.59}$$

The last column of $\hat{\mathbf{H}}_0(z)$ and the last row of $\hat{\mathbf{H}}_1(z)$ were artificially added to generate a square circulant matrix in the sequel whose dimension can be designed to be a power of two, allowing the use of FFTs. The overall factorization of $\hat{\mathbf{H}}(z)$ as above described is crucial to derive the frequency-domain algorithm and the MDF in the sequel. It is worth noting that our presentation follows the embedding approach which was generalized in [41], and was indirectly employed in [42]. The embedding approach leads to a simpler derivation than those presented in early references [35]-[40].

The embedding approach starts by defining a circulant matrix $\hat{\mathbf{H}}_2(z)$ as follows

$$\hat{\mathbf{H}}_2(z) = \begin{bmatrix} \hat{H}_0(z) & \hat{H}_1(z) & \hat{H}_2(z) & 0 & 0 & 0 \\ 0 & \hat{H}_0(z) & \hat{H}_1(z) & \hat{H}_2(z) & 0 & 0 \\ 0 & 0 & \hat{H}_0(z) & \hat{H}_1(z) & \hat{H}_2(z) & 0 \\ 0 & 0 & 0 & \hat{H}_0(z) & \hat{H}_1(z) & \hat{H}_2(z) \\ \hat{H}_2(z) & 0 & 0 & 0 & \hat{H}_0(z) & \hat{H}_1(z) \\ \hat{H}_1(z) & \hat{H}_2(z) & 0 & 0 & 0 & \hat{H}_0(z) \end{bmatrix} \tag{12.60}$$

The matrix $\hat{\mathbf{H}}_0(z)$ is embedded into $\hat{\mathbf{H}}_2(z)$, that is:

$$\hat{\mathbf{H}}_0(z) = \begin{bmatrix} \mathbf{I}_L & \mathbf{0} \end{bmatrix} \hat{\mathbf{H}}_2(z) \tag{12.61}$$

where in the above equation we treat the general case, i.e., for block length equal to L instead of 3. Since the matrix $\hat{\mathbf{H}}_2(z)$ is circulant, it can be diagonalized by a DFT matrix as follows

$$\hat{\mathbf{H}}_2(z) = \mathcal{F}^* \mathbf{W}(z) \mathcal{F} \tag{12.62}$$

where $\mathbf{W}(z)$ is a diagonal matrix. If these diagonal elements are given by single complex coefficients, the resulting algorithm is the so-called frequency-domain algorithm, whereas for higher order filters the resulting algorithm is called MDF.

From equations (12.58), (12.61) and (12.62), we can relate the blocked matrix of the overall adaptive filter to the adaptive filter in the bins as follows

$$\hat{\mathbf{H}}(z) = \begin{bmatrix} \mathbf{I}_L & \mathbf{0} \end{bmatrix} \mathcal{F}^* \mathbf{W}(z) \mathcal{F} \hat{\mathbf{H}}_1(z) \tag{12.63}$$

In the frequency domain, the block output is given by

$$\mathcal{Z}[\mathbf{y}(m)] = \hat{\mathbf{H}}(z)\mathcal{Z}[\mathbf{x}(m)] \tag{12.64}$$

whereas the error signal vector is given by

$$\mathcal{Z}[\mathbf{e}(m)] = \mathcal{Z}[\mathbf{d}(m)] - \mathcal{Z}[\mathbf{y}(m)] \tag{12.65}$$

We use as an objective function the squared values of the error vector elements, that is

$$\xi = \sum_{i=0}^{L-1} |e_i(m)|^2 \tag{12.66}$$

In problem 16, the resulting gradient estimate for the set of coefficients placed at each bin is shown to be given by

$$\begin{aligned}\hat{\mathbf{g}}_{\mathbf{W},i}(m) &= -2\mathbf{u}_i^*(m)\left(\mathcal{F}\begin{bmatrix}\mathbf{I}_L\\ \mathbf{0}\end{bmatrix}\mathbf{e}(m)\right)_i \\ &= -2\mathbf{u}_i^*(m)\left(\tilde{\mathbf{e}}(m)\right)_i \\ &= -2\mathbf{u}_i^*(m)\tilde{e}_i(m)\end{aligned} \tag{12.67}$$

where $\mathbf{u}_i^*(m)$ represents the complex conjugate of the data vector stored in ith bin, at instant m, and $(\tilde{\mathbf{e}}(m))_i$ denotes the ith element of vector $\tilde{\mathbf{e}}(m)$ with

$$\tilde{\mathbf{e}}(m) = \mathcal{F}\begin{bmatrix}\mathbf{I}_L\\ \mathbf{0}\end{bmatrix}\mathbf{e}(m)$$

It is worth mentioning that the data vectors are calculated as follows

$$\mathcal{Z}\begin{bmatrix}\mathbf{u}_0^T(m)\\ \vdots \\ \mathbf{u}_{2L-1}^T(m)\end{bmatrix} = \mathcal{F}\hat{\mathbf{H}}_1(z)\mathcal{Z}\left[\mathbf{x}(m)\cdots\mathbf{x}(m-N_s+1)\right] \tag{12.68}$$

In this case, the NLMS updating equation is given by

$$\mathbf{w}_i(m+1) = \mathbf{w}_i(m) + \frac{2\mu}{\gamma+\sigma_i^2(m)}\mathbf{u}_i^*(m)\tilde{e}_i(m) \tag{12.69}$$

for $i = 0, 1, \ldots, N_s$, where N_s is the length of the adaptive filter at the output of bin i, and $\sigma_i^2(m) = (1-\alpha)\sigma_i^2(m-1) + \alpha\,|u_i(m)|^2$, with $0 < \alpha \leq 0.1$ and γ is a small constant as established before.

If we examine the first row of the matrices in equation (12.62) and use the fact that $\mathcal{F}$ is a symmetric matrix, it is straightforward to infer that

$$\begin{bmatrix} \hat{H}_0(z) \\ \hat{H}_1(z) \\ \vdots \\ \hat{H}_{L-1}(z) \\ 0 \\ \vdots \\ 0 \end{bmatrix} = \frac{1}{\sqrt{2L}} \mathcal{F} \begin{bmatrix} W_0(z) \\ W_1(z) \\ \vdots \\ W_{2L-1}(z) \end{bmatrix} \tag{12.70}$$

where $W_i(z)$, for $i = 0, 1, \ldots, 2L-1$, are the transfer functions of the subfilters of $\mathbf{W}(z)$. The above equation shows that the adaptive filters in the bins must be constrained such that $\hat{\mathbf{H}}_2(z)$ contains the estimates of the polyphase components of the unknown system. Note that, in the update equation (12.69), it is not guaranteed that this constraint is satisfied.

As a solution, we can enforce the constraint in the adaptive-filter updating with the help of equation (12.70), as follows. First define the matrices that include all the coefficients and data of all subfilters:

$$\begin{aligned} \boldsymbol{\mathcal{W}}(m) &= \begin{bmatrix} \mathbf{w}_0^T(m) \\ \mathbf{w}_1^T(m) \\ \vdots \\ \mathbf{w}_{2L-1}^T(m) \end{bmatrix} \\ \boldsymbol{\mathcal{U}}(m) &= \begin{bmatrix} \mathbf{u}_0^H(m) \\ \mathbf{u}_1^H(m) \\ \vdots \\ \mathbf{u}_{2L-1}^H(m) \end{bmatrix} \end{aligned} \tag{12.71}$$

and a diagonal matrix $\boldsymbol{\mathcal{E}}(m)$ whose nonzero elements are the entries of vector $\tilde{\mathbf{e}}(m)$.

In matrix form the updating equation (12.69) can be rewritten as

$$\boldsymbol{\mathcal{W}}(m+1) = \boldsymbol{\mathcal{W}}(m) + 2\mu \boldsymbol{\Sigma}^{-2}(m) \boldsymbol{\mathcal{E}}(m) \boldsymbol{\mathcal{U}}(m) \tag{12.72}$$

where $\boldsymbol{\Sigma}^{-2}(m)$ is a diagonal matrix whose elements are $\frac{1}{\gamma + \sigma_i^2(m)}$, with $\sigma_i^2(m) = (1-\alpha)\sigma_i^2(m-1) + \alpha |u_i(m)|^2$.

A constrained version of the above equation can be derived by observing equation (12.70). The resulting algorithm consists of enforcing the constraint in the update equation as follows (see problem 17)

$$\boldsymbol{\mathcal{W}}_c(m+1) = \mathcal{F}^* \begin{bmatrix} \mathbf{I}_L \\ \mathbf{0} \end{bmatrix} \begin{bmatrix} \mathbf{I}_L & \mathbf{0} \end{bmatrix} \mathcal{F} \boldsymbol{\mathcal{W}}(m+1) \tag{12.73}$$

The above algorithm is widely known as the constrained frequency-domain algorithm. The original constrained algorithm was derived for a single coefficient per bin, not for the more general MDF.

Also, the particular version of the algorithm presented here corresponds to the overlap-save version, in which the constraints are included in order to guarantee that the internal DFTs perform linear convolutions on the signals involved. By examining equation (12.63), the reader should note that the transform applied to the input signal after it is filtered by $\hat{\mathbf{H}}_1(z)$ has length $2L$, whereas in the calculation of the adaptive-filter output block, L signals are discarded due to the product by $[\mathbf{I}_L \ \mathbf{0}]$. This reflects the overlap-save characteristic of the algorithm. The block diagram related to this algorithm is depicted in Fig. 12.26.

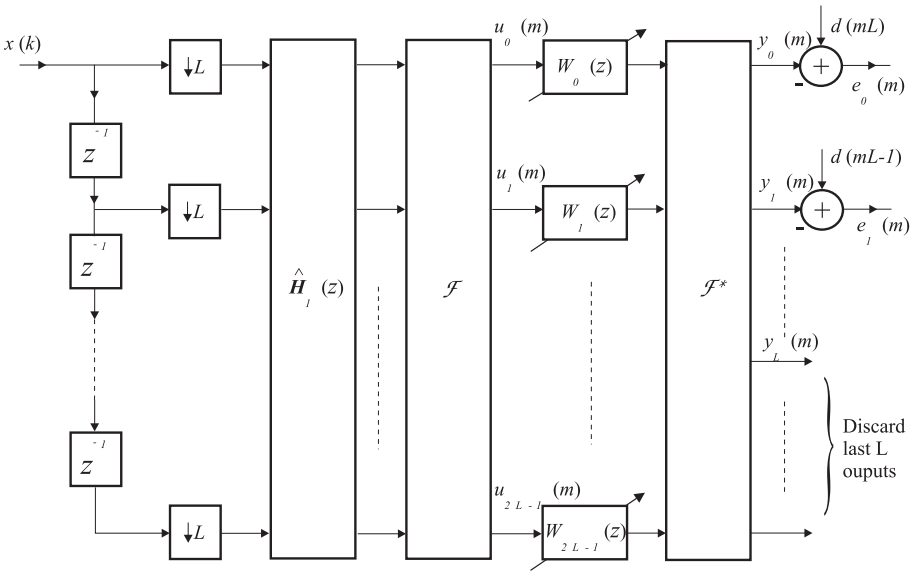

Figure 12.26 Frequency-domain adaptive-filtering structure.

The description of the constrained frequency-domain algorithm is detailed in Algorithm 12.4. Likewise, an overlap-add version of the constrained frequency domain algorithm also exists, and interested readers should refer to [36], [41] (see problem 18).

It is worth mentioning that a delayless version of the constrained frequency-domain algorithm follows directly from equation (12.70) which implements the mapping from the subband filter to the polyphase components of the fullband estimate. It is also important to note that although the embedding approach presented here was based on the DFT, it can also be employed using other class of transforms such as DCT, DST and Hartley transform. Though these alternative transforms require more cumbersome embedding formulations, they do not require complex arithmetic when environment signals are not represented by complex numbers [41].

Example 12.4

Repeat example 12.1 using the multidelay structure with $L = 64$ and the frequency-domain structure. Choose the appropriate order for the subfilters in the multidelay case.

Algorithm 12.4

Constrained Frequency-Domain Algorithm

Initialization

$\gamma =$ small constant

$0 < \alpha \leq 0.1$

Do for each $x(iL)$ and $d(iL)$ given, for $i \geq 0$

$$\begin{bmatrix} \mathbf{u}_0^T(m) \\ \vdots \\ \mathbf{u}_{2L-1}^T(m) \end{bmatrix} = \mathcal{F}\hat{\mathbf{H}}_1(z)\,[\mathbf{x}(m) \cdots \mathbf{x}(m-N_s+1)]$$

the dimension of $\mathcal{F}$ is $2L$.

$$\mathbf{e}(m) = \mathbf{d}(m) - \begin{bmatrix} \mathbf{I}_L & \mathbf{0} \end{bmatrix} \mathcal{F}^* \begin{bmatrix} \mathbf{w}_{c,0}^T(m)\mathbf{u}_0^*(m) \\ \mathbf{w}_{c,1}^T(m)\mathbf{u}_1^*(m) \\ \vdots \\ \mathbf{w}_{c,2L-1}^T(m)\mathbf{u}_{2L-1}^*(m) \end{bmatrix}$$

where $\mathbf{w}_{c,l}$ are the constrained adaptive-filter coefficients of the $(l-1)$th subband, that is the $(l-1)$th row of $\boldsymbol{\mathcal{W}}_c(m)$.

$$\tilde{\mathbf{e}}(m) = \mathcal{F} \begin{bmatrix} \mathbf{I}_L \\ \mathbf{0} \end{bmatrix} \mathbf{e}(m)$$

$$\sigma_i^2(m) = (1-\alpha)\sigma_i^2(m-1) + \alpha\,|u_i(m)|^2$$

$$\boldsymbol{\mathcal{W}}(m+1) = \boldsymbol{\mathcal{W}}(m) + 2\mu\boldsymbol{\Sigma}^{-2}(m)\boldsymbol{\mathcal{E}}(m)\boldsymbol{\mathcal{U}}(m)$$

$$\boldsymbol{\mathcal{W}}_c(m+1) = \mathcal{F}^* \begin{bmatrix} \mathbf{I}_L \\ \mathbf{0} \end{bmatrix} \begin{bmatrix} \mathbf{I}_L & \mathbf{0} \end{bmatrix} \mathcal{F}\boldsymbol{\mathcal{W}}(m+1)$$

Solution:

For the frequency-domain algorithm we use a block size of 90 and the following parameters: $\alpha = 0.5$, $\gamma = 0.001$, and $\mu = 0.2$. The average MSE obtained from five runs is -29.2 dB.

Fig. 12.27 depicts the global MSE where the algorithm converges rather fast to the minimum MSE. Fig. 12.28 shows that the magnitude response obtained after convergence approaches the unknown system response.

For the multidelay filter, we use a block size of 18 with five coefficients in each bin and the following parameters: $\alpha = 0.1$, $\gamma = 0.001$, and $\mu = 0.4$. The average MSE obtained from five runs is -29.0 dB. Fig. 12.29 depicts the global MSE where we observe that the MDF algorithm also converges fast to the minimum MSE. Fig. 12.30 shows that the magnitude response obtained after convergence does not approach so closely the unknown system response.

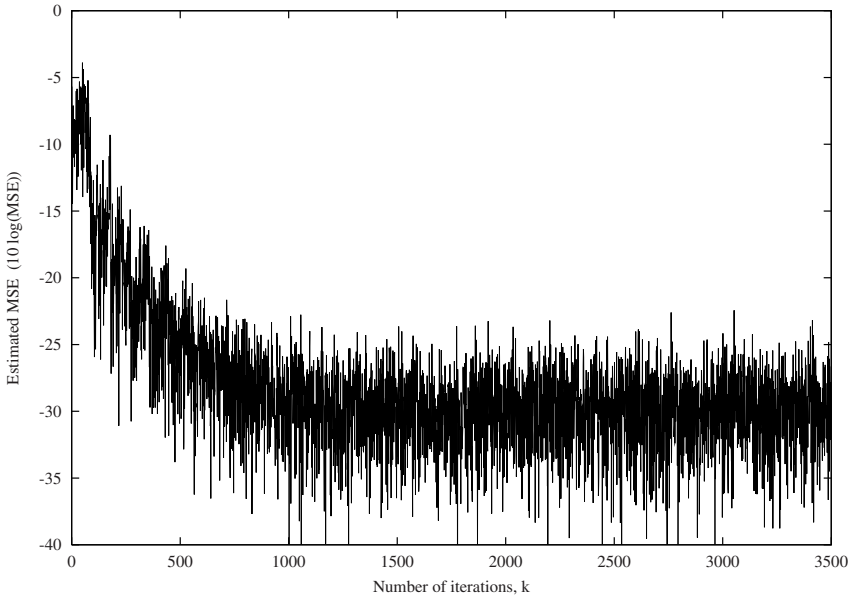

Figure 12.27 Global error of the frequency-domain structure.

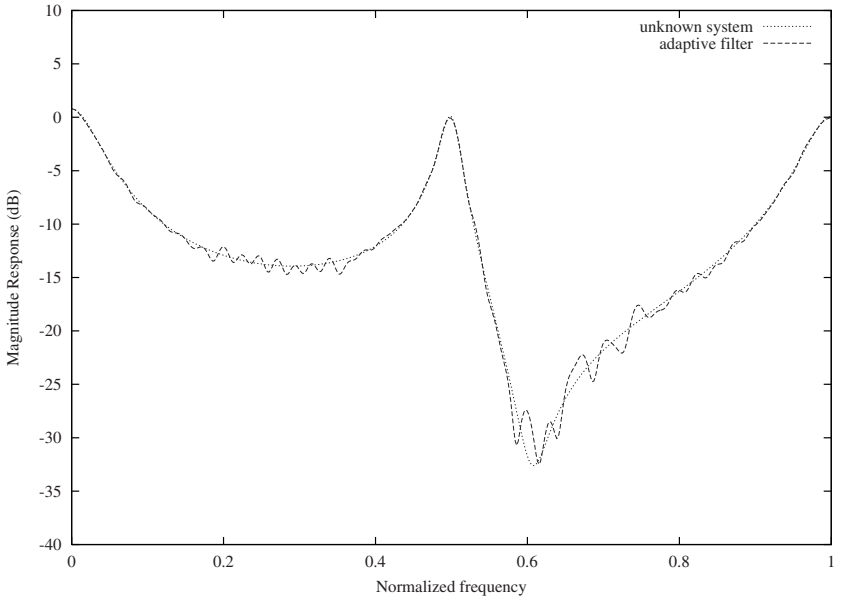

Figure 12.28 Magnitude responses of the unknown system and the obtained model at a given iteration.

□

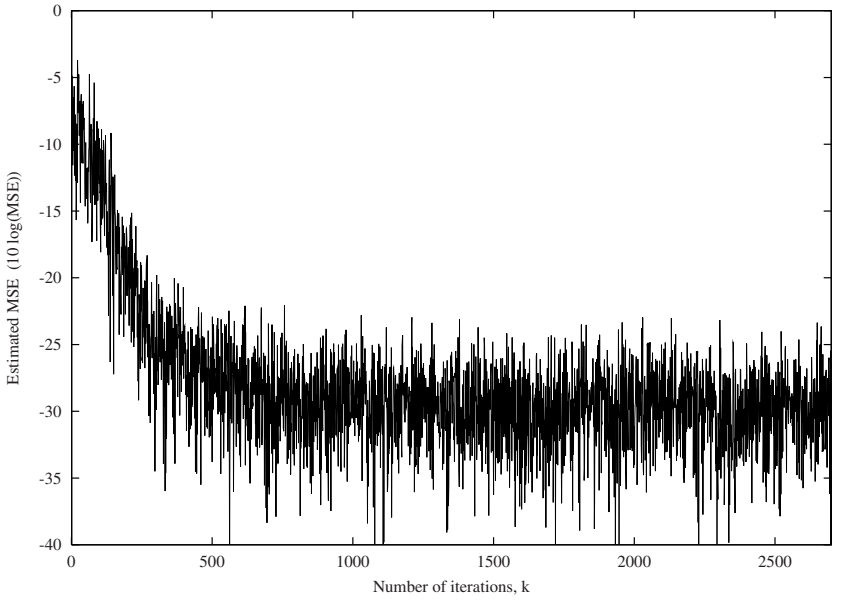

Figure 12.29 Global error of the MDF structure.

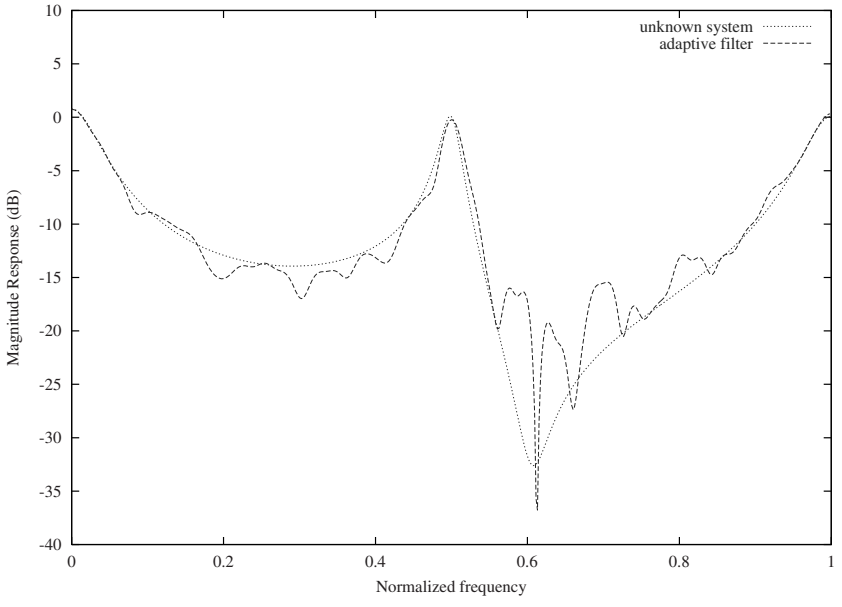

Figure 12.30 Magnitude responses of the unknown system and the obtained model at a given iteration, MDF case.

12.8 CONCLUSION

Subband adaptive filters are viable solutions to reduce the high-computational complexity inherent in applications where long-impulse-response models are required. In addition, the effective split of the internal signals into subbands leads to fast convergence.

This chapter presented several subband structures. After a brief introduction to multirate systems, we discussed the design of two-band and M-band perfect reconstruction filter banks. The subband adaptive filters using local subband errors, leading to the open-loop structure, were described. The closed-loop subband filters, which make use of the global error, were also introduced. We presented a special type of filter bank which aims to eliminate cross adaptive filters and utilizes fractional delays.

Another type of subband adaptive filter is based on a delayless structure. In this structure, the adaptive-filter coefficient updating is performed in subbands and a subband to fullband mapping allows the input signal to be filtered in fullband. This strategy avoids the signal path delay introduced by the filter bank. Also, we presented expressions to estimate the computational complexity of the subband adaptive filters.

Finally, we presented the frequency-domain and multidelay structures, which employ block processing and are closely related to subband adaptive filters. These structures further lead to reduced computational complexity.

12.9 REFERENCES

1. A. Gilloire, "Experiments with sub-band acoustic echo cancellers for teleconferencing," *Proc. IEEE Intern. Conf. Acoust., Speech, Signal Processing*, pp. 2141-2144, Dallas, TX, April 1987.

2. A. Gilloire and M. Vetterli, "Adaptive filtering in subbands with critical sampling: analysis, experiments, and application to acoustic echo cancellation," *IEEE Trans. on Signal Processing*, vol. 40, pp. 1862-1875, Aug. 1992.

3. W. Kellermann, "Analysis and design of multirate systems for cancellation of acoustical echoes," *Proc. IEEE Intern. Conf. Acoust., Speech, Signal Processing*, pp. 2570-2573, New York, NY, April 1988.

4. Y. Lu and J. M. Morris, "Gabor expansion for adaptive echo cancellation," *IEEE Signal Processing Magazine*, vol.16, pp. 68-80, March 1999.

5. E. Hänsler and G. U. Schmidt, "Hands-free telephones - joint control of echo cancellation and post filtering," *Signal Processing*, vol. 80, pp. 2295-2305, Nov. 2000.

6. M. R. Petraglia and S. K. Mitra, "Performance analysis of adaptive filter structures based on subband decomposition," *Proc. IEEE Intern. Symp. on Circuits and Systems*, pp. 60-63, Chicago, IL, May 1993.

7. P. L. De León, II and D. M. Etter, "Experimental results with increased bandwidth analysis filters in oversampled, subband acoustic echo cancellers," *IEEE Signal Processing Letters*, vol. 2, pp. 1-3, Jan. 1995.

8. E. A. B. da Silva and P. S. R. Diniz, "Time-Varying Filters," *Encyclopedia of Electrical and Electronics Engineering*, Editor: John G. Webster, John Wiley & Sons, New York, NY, vol. 22, pp. 249-274, 1999.

9. P. P. Vaidyanathan, *Multirate Systems and Filter Banks*, Prentice-Hall, Englewood Cliffs, NJ, 1993.

10. M. Vetterli and J. Kovačević, *Wavelets and Subband Coding*, Prentice-Hall, Englewood Cliffs, NJ, 1995.

11. H. Bölcskei and F. Hlawatsch, "Oversampled cosine modulated filter banks with perfect reconstruction," *IEEE Trans. on Signal Processing*, vol. 45, pp. 1057-1071, Aug. 1998.

12. V. P. Sathe and P. P. Vaidyanathan, "Effects of multirate systems on the statistical properties of random signals," *IEEE Trans. on Signal Processing*, vol. 41, pp. 131-146, Jan. 1993.

13. Y. G. Yang, N. I. Cho, and S. U. Lee, "On the performance analysis and applications of subband adaptive digital filters," *Signal Processing*, vol. 41, pp. 295-307, 1995.

14. M. R. Petraglia, R. G. Alves, and P. S. R. Diniz, "New structures for adaptive filtering in subbands with critical sampling," *IEEE Trans. on Signal Processing*, vol.48 , pp. 3316-3327, Dec. 2000.

15. M. R. Petraglia, R. G. Alves, and P. S. R. Diniz, "Convergence analysis of an oversampled subband adaptive filtering structure with local errors," *Proc. IEEE Intern. Symp. on Circuits and Systems*, pp. I-563-I-566, Geneve, Switzerland, May 2000.

16. M. R. Petraglia, R. G. Alves, and P. S. R. Diniz, "Convergence analysis of an oversampled subband adaptive filtering structure with global error," *Proc. IEEE Intern. Conf. Acoust., Speech, Signal Processing*, pp. 468-471, Istanbul, Turkey, June 2000.

17. J. R. Treichler, S. L. Wood, and M. G. Larimore, "Convergence rate limitations in certain frequency-domain adaptive filters," *Proc. IEEE Intern. Conf. Acoust., Speech, Signal Processing*, pp. 960-963, Scotland, May 1989.

18. G. Strang, *Linear Algebra and Its Applications*, Academic Press, New York, NY, 1980.

19. S. S. Pradhan and V. U. Reddy, "A new approach to subband adaptive filtering," *IEEE Trans. on Signal Processing*, vol. 47, pp. 655-664, March 1999.

20. Y. Higa, H. Ochi, and S. Kinjo,"A subband adaptive filter with the statistically optimum analysis filter bank," *IEEE Trans. on Circuits and Systems II: Analog and Digital Signal Processing*, vol. 45, pp. 1150-1154, Aug. 1998.

21. S. M. Kuo and D. R. Morgan, *Active Noise Control Systems*, John Wiley & Sons, New York, NY, 1996.

22. D. R. Morgan and M. J. C. Thi, "A delayless subband adaptive filter architecture," *IEEE Trans. on Signal Processing*, vol. 43, pp. 1819-1830, Aug. 1995.

23. R. Merched, P. S. R. Diniz, and M. R. Petraglia, "A delayless alias-free subband adaptive filter structure," *IEEE Trans. on Signal Processing*, vol. 47, pp. 1580-1591, June 1999.

24. R. Merched, P. S. R. Diniz, and M. R. Petraglia, "A delayless alias-free subband adaptive filter structure," *Proc. 1997 IEEE Intern. Symposium on Circuits and Systems*, Hong-Kong, pp. 2329-2332, June 1997.

25. N. Hirayama, H. Sakai, and S. Miyagi, "Delayless subband adaptive filtering using the Hadamard transform," *IEEE Trans. on Signal Processing*, vol. 47, pp. 1731-1734, June 1999.

26. S. Ohno and H. Sakai, "On Delayless subband adaptive filtering by subband/fullband transforms," *IEEE Signal Processing Letters*, vol. 6, pp. 236-239, Sept. 1999.

27. K. Nishikawa and H. Kiya, "Conditions for convergence of a delayless subband adaptive filter and its efficient implementation," *IEEE Trans. on Signal Processing*, vol. 46, pp. 1158-1167, April 1998.

28. U. Iyer, M. Nayeri, and H. Ochi,"Polyphase based adaptive structure for adaptive filtering and tracking," *IEEE Trans. on Circuits and Systems II: Analog and Digital Signal Processing*, vol. 43, pp. 220-232, March 1996.

29. F. G. V. Resende, Jr., P. S. R. Diniz, K. Tokuda, M. Kaneko, and A. Nishihara, "LMS-based algorithms with multi-band decomposition of the estimation error applied to system identification," *IEICE Trans. Fundamentals*, Special Issue on Digital Signal Processing, Japan, vol. E00-A, pp. 1376-1383, Aug. 1997.

30. F. G. V. Resende, Jr., P. S. R. Diniz, K. Tokuda, M. Kaneko, and A. Nishihara, "New adaptive algorithms based on multi-band decomposition of the error signal," *IEEE Trans. on Circuits and Systems II: Analog and Digital Signal Processing*, vol. 45, pp. 592-599, May 1998.

31. T. I. Laakso, V. Välimäki, M. Karjalainen, and U. K. Laine, "Splitting the unit delay," *IEEE Signal Processing Magazine*, vol.13, pp. 30-60, Jan. 1996.

32. I.-S. Lin and S. K. Mitra,"Overlapped block digital filtering," *IEEE Trans. on Circuits and Systems II: Analog and Digital Signal Processing*, vol. 43, pp. 586-596, Aug. 1996.

33. P. S. R. Diniz, E. A. B. da Silva, and S. L. Netto, *Digital Signal Processing: System Analysis and Design*, Cambridge University Press, New York, NY, 2002.

34. G. A. Clark, S. R. Parker, and S. K. Mitra, "A unified approach to time- and frequency-domain realization of FIR adaptive digital filters," *IEEE Trans. on Acoust., Speech, Signal Processing*, vol. ASSP-31, pp. 1073-1083, Oct. 1983.

35. P. C. Sommen, "On the convergence properties of a partitioned block frequency domain adaptive filter (PBFDAF)," *Proc. European Signal Processing Conf.*, pp. 201-203, Barcelona, Spain, Sept. 1990.

36. J. J. Shynk, "Frequency-domain and multirate adaptive filtering," *IEEE Signal Processing Magazine*, vol. 9, pp. 15-37, Jan. 1992.

37. J.-S. Soo and K. Pang, "Multidelay block frequency domain adaptive filter," *IEEE Trans. on Acoust., Speech, Signal Processing*, vol. 38, pp. 373-376, Feb. 1990.

38. B. Fahang-Boroujeny, "Analysis and efficient implementation of partitioned block LMS filters," *IEEE Trans. on Signal Processing*, vol. 44, pp. 2865-2868, Nov. 1996.

39. E. Moulines, O. A. Amrane, and Y. Grenier, "The generalized multidelay adaptive filter: structure and convergence analysis," *IEEE Trans. on Signal Processing*, vol. 43, pp. 14-28, Jan. 1995.

40. M. de Couville and P. Duhamel, "Adaptive filtering in subbands using a weighted criterion," *IEEE Trans. on Signal Processing*, vol. 46, pp. 2359-2371, Sep. 1998.

41. R. Merched and A. H. Sayed, "An embedding approach to frequency-domain and subband adaptive filtering," *IEEE Trans. on Signal Processing*, vol. 48, pp. 2607-2619, Sept. 2000.

42. K. Eneman and M. Moonen, "Hybrid subband/frequency-domain adaptive filters," *Signal Processing*, vol. 81, pp. 117-136, 2001.

12.10 PROBLEMS

1. Show the validity of equation (12.1).

2. Design a linear-phase two-band filter bank of order 42 using the approach described in subsection 12.3.1.

3. Design a uniform linear-phase 8-band filter bank having at least 40dB of stopband attenuation, using a hierarchical filter bank.

4. Design a uniform 8-band filter bank having at least 40dB of stopband attenuation, using the cosine-modulated method.

5. Design a fractional delay via a Nyquist filter having at least 60dB of stopband attenuation.

6. Use an open-loop subband adaptive filter with four bands to identify a system with the transfer function given below. The input signal is a uniformly distributed white noise with variance $\sigma_x^2 = 1$, and the measurement noise is Gaussian white noise uncorrelated with the input with variance $\sigma_n^2 = 10^{-3}$. The filter bank is a cosine-modulated type of length 64.

$$H(z) = \frac{0.1z}{(z + 0.9)} + \frac{0.1z}{(z - 0.9)}$$

   Choose the order of the equivalent FIR filter as the one for which the envelop of the unknown system impulse response falls below $\frac{1}{1000}$ of its leading term. Plot the MSE for an average of five independent runs, including the local errors and the overall error.

7. Repeat the previous problem using a closed-loop algorithm and interpret the results.

8. Show that the recursive equation governing the convergence of the adaptive coefficients in the closed-loop structure has the characteristic polynomial of equation (12.36).

9. For a prototype filter of length 256, and 32 subbands, calculate and plot the ratio between the computational complexities of the subband and fullband implementations, for $N = 256, 512, 1024, 2048$, and 4096. Consider the maximally decimated case as well as the cases where $L = M - 1$, $L = \frac{3M}{4}$, and $L = \frac{M}{2}$. Assume we are using a simple DFT filter bank (which is similar to the filter bank using fractional delays where these delays are replaced by a transfer function equal to one) and consider the cases of open-loop and closed-loop structures.

10. Replace the structure in problem 6 by the closed-loop and open-loop delayless structures with the fractional delays designed via a Nyquist filter of order 64.

11. In a system identification problem, the input signal is a uniformly distributed white noise with variance $\sigma_{n_x}^2 = 0.1$, filtered by an all-pole filter given by

$$H_{n_x}(z) = \frac{z}{z - 0.95}$$

    The unknown system is a 300th-order FIR filter whose impulse response is identical to the first 301 impulse response samples of the transfer function described by

$$H(z) = \frac{0.00756z^2}{(z^2 - 1.960636z + 0.9849357)}$$

    Choose the appropriate parameters, run an ensemble of 5 experiments, and plot the average learning curve. Use the delayless subband filter using fractional delays in the open-loop scheme, with 8-bands.

12. Repeat problem 11 using the closed-loop structure.

13. Prove that the expressions for the computational complexity of the subband adaptive filters in equations (12.52) to (12.56) are valid.

14. Solve problem 6 using the frequency-domain structure with $L = 64$.

15. Solve problem 6 using the multidelay structure with $L = 16$. Choose the appropriate order for the subfilters.

16. Prove the validity of equations (12.67), (12.68), and (12.70). Hint: Create a block-diagonal matrix of subband input signals consisting of

$$\text{diag}\{\mathbf{u}_0^T(m)\ \ \mathbf{u}_1^T(m)\ \ \cdots\ \ \mathbf{u}_{2L-1}^T(m)\}$$

and a vector containing all the elements of the subband adaptive filters

$$\begin{bmatrix} \mathbf{w}_0(m) \\ \mathbf{w}_1(m) \\ \vdots \\ \mathbf{w}_{2L-1}(m) \end{bmatrix}$$

17. Demonstrate how the relation below enforces the constraint of equation (12.70).

$$\mathcal{F}^* \begin{bmatrix} \mathbf{I}_L \\ \mathbf{0} \end{bmatrix} \begin{bmatrix} \mathbf{I}_L & \mathbf{0} \end{bmatrix} \mathcal{F}$$

18. Derive an overlap-add version of the frequency-domain algorithm using the embedding strategy in which a 3×3 matrix $\hat{\mathbf{H}}(z)$ can be written as

$$\hat{\mathbf{H}}(z) = \hat{\mathbf{H}}_3(z)\hat{\mathbf{H}}_4(z)$$

where

$$\hat{\mathbf{H}}_3(z) = \begin{bmatrix} 0 & 0 & 1 & 0 & 0 \\ z^{-1} & 0 & 0 & 1 & 0 \\ 0 & z^{-1} & 0 & 0 & 1 \end{bmatrix}$$

$$\hat{\mathbf{H}}_4(z) = \begin{bmatrix} \hat{H}_2(z) & 0 & 0 \\ \hat{H}_1(z) & \hat{H}_2(z) & 0 \\ \hat{H}_0(z) & \hat{H}_1(z) & \hat{H}_2(z) \\ 0 & \hat{H}_0(z) & \hat{H}_1(z) \\ 0 & 0 & \hat{H}_0(z) \end{bmatrix}$$